Next Materials 11 (2026) 101971

Contents lists available at ScienceDirect

Next Materials

journal homepage: www.sciencedirect.com/journal/next-materials

Review article

Machine learning-driven optimization of biochar-based supercapacitors for sustainable energy storage: Mechanisms, trends, and perspectives

Fatima Sajjad [a], Rashid Iftikhar [a,*], Muhammad Ali Inam [a,b], Saifullah Zadran [c], Salman Haider [d], Sahar Saleem [e], Humayun Nadeem [f], Alim-un-Nisa [g]

[a] Institute of Environmental Sciences and Engineering, School of Civil and Environmental Engineering, National University of Sciences and Technology, Islamabad 44000, Pakistan
[b] Institute for Water Resources and Water Supply, Hamburg University of Technology (TUHH), Am Schwarzenberg-Campus 3, Hamburg 21073, Germany
[c] Department of Robotics and Artificial Intelligence, School of Mechanical and Manufacturing Engineering, NUST, Islamabad, Pakistan
[d] Faculty of Software Engineering, Torrens University, Sydney, Australia
[e] Department of Sciences, School of Interdisciplinary Engineering & Science (SINES), National University of Science and Technology (NUST), Islamabad, Pakistan
[f] School of Chemical and Materials Engineering (SCME), National University of Sciences and Technology (NUST), Islamabad 44000, Pakistan
[g] Food and Biotechnology Research Centre, Pakistan Council of Scientific and Industrial Research, Lahore, Pakistan

ARTICLE INFO

Keywords:
Carbon electrode modification
Heteroatom doping
Nanocomposite engineering
Predictive modeling
Electrochemical energy storage

ABSTRACT

Global transition toward sustainable and efficient energy storage has intensified research into supercapacitors, valued for their rapid charge-discharge capability, high power density, and long operational lifespan. Among carbonaceous materials, biomass-derived biochar has emerged as a low-cost, renewable, and structurally tunable precursor for electrode design. This review provides a structured and critical synthesis of biochar-based supercapacitor strategies, systematically categorizing heteroatom doping, nanocomposite engineering, and hybrid architecture within an integrated electrochemical performance framework. Unlike existing literature that predominantly summarizes modification approaches, this review emphasizes cross-study comparability, mechanistic attribution, and device-level relevance to clarify transferable design principles. A consolidated analysis of recent machine learning (ML) applications reveals a paradigm shift from empirical optimization to data-driven predictive design. Benchmarking against reported datasets, descriptors, and model architectures, we confirm that tree-based ensemble and neural-network models (e.g., XGBoost, LightGBM, ANN) consistently achieve high predictive accuracy ($R^2 > 0.9$), while also identifying current limitations in data standardization and descriptor harmonization. The review critically evaluates how ML can move beyond correlation towards interpretable and transferable optimization under realistic device constraints.

Finally, a converging research roadmap is proposed, prioritizing standardized reporting, device-level benchmarking, and constraint-aware ML integration to accelerate scalable implementation. By integrating materials engineering, data-driven modeling, and practical deployment considerations, this review establishes a comprehensive framework for advancing sustainable biochar-based supercapacitors toward real-world energy storage applications.

1. Introduction

The swift progression of emerging technologies has led to a rise in global energy demand, accompanied by escalating concerns over fossil fuel depletion and the deterioration of natural environment. Although renewable energy options such as wind and solar power have progressed considerably, their intermittent nature necessitates the development of reliable and high-efficiency energy storage systems. Systems capable of meeting the escalating energy requirements resulting from worldwide population growth [1]. Continuous development and exploration of sustainable energy storage technologies is vital for replacing fossil fuel-based energy systems. Among novel solutions, supercapacitors have gained remarkable prominence due to their superior power density, safety, cycling stability, and reversibility [2,3]. Owing to their rapid charging capability and excellent power performance, supercapacitors are increasingly used in portable electronics and electric transportation

* Corresponding author.
E-mail addresses: rashid.iftikhar@iese.nust.edu.pk, rashid.iftikhar@hotmail.com (R. Iftikhar).

https://doi.org/10.1016/j.nxmate.2026.101971
Received 27 December 2025; Received in revised form 3 March 2026; Accepted 23 March 2026
Available online 31 March 2026

systems [4,5]. Like rechargeable batteries, supercapacitors belong to the class of electrochemical energy storage devices (EESDs), that is they rely on ion diffusion and migration mechanisms to store and transform energy. Supercapacitors typically contain two electrodes divided by an ion-permeable separator that permits ion transport while inhibiting electron transfer, whereas the electrolyte provides a conductive medium for ion transfer between the electrodes [6,7]. Supercapacitors have various benefits, including rapid charging and switching, long cycle life, and significant power density. The electrode itself, electrolyte, and electrode-electrolyte interactions all have an impact on supercapacitor properties. The overall storage capability of a supercapacitor depends on interfacial charge accumulation, highlighting the importance of electrode material in their performance.

Carbon-based materials are considered as one of the leading candidates for constructing supercapacitor electrodes due to their surface area, chemical robustness, electrical conductivity, and economic feasibility [8]. Among carbon sources, biomass-based carbon stands out as a renewable, carbon-neutral resource with low environmental impact and reduced carbon dioxide emissions [9]. Biomass can be transformed into porous carbon structures such as biochar through pyrolysis, which has attracted increasing attention for its inherently large surface area, hierarchical pore network, adjustable surface functionalities, and capacity for heteroatom doping [10–12]. Compared to other materials, biochar also offers additional advantages such as environmental sustainability, cost-effectiveness, reusability, and facile synthesis [13]. The physico-structural properties of biochar, particularly particle size, strongly influence its subsequent modification behavior. Depending on the pyrolysis method and operational parameters, biochar particles may vary in size ranging from micrometers to centimeters [14]. Recently, nano-biochar has emerged as an innovative subclass of biomass-based carbon materials that combine the advantages of biochar and nanostructured systems. At particle sizes below 100 nm, the markedly increased surface to volume ratio leads to higher surface energy and adsorption capacity [15–17]. Nanoscale enhancement enables modification processes, such as heteroatom incorporation and composite development, to be carried out more efficiently.

The post-synthesis engineering of biochar is a primary factor that defines the electrochemical behavior of an electrode, independent of the biomass source, its intrinsic purity and the pyrolysis conditions. Broadly, two modification strategies have been reported in literature with rare overlaps. The first deals with activation and structural modification involving chemical and physical treatments to improve the surface functions and pore accessibility. These treatments are often combined with nanocomposite inclusion to improve conductivity and catalytic behavior. The second focuses on heteroatom doping, where elements such as sulfur, nitrogen, phosphorus, or boron are introduced into the carbon structure to alter charge distribution, electronic configuration, and surface polarity. While structural modification and electronic configuration are two distinct modification strategies, they occasionally overlap and collectively describe biochar design for electrochemical applications. Despite a great deal of research into the modification processes for biochar-based materials, an in-depth analysis that connects the performance of biochar-based electrode materials with cutting-edge AI and machine learning methods is still missing.

To systematically address this shortcoming, the present review is structured into four primary objectives. First, establish an integrated structural electrochemical performance framework that systematically links biochar modification strategies to device-level metrics. Second, critically compare heteroatom doping and nanocomposite engineering through mechanistic attribution and cross-study benchmarking to identify transferable design principles. Third, evaluate current machine learning approaches by analyzing dataset scope, descriptor selection, model interpretability, and predictive reliability, highlighting both capabilities and limitations. Finally, we propose a converging research roadmap that aligns materials design, device validation, and constraint-aware ML optimization under realistic scalability and manufacturing considerations. By explicitly bridging materials science and artificial intelligence within a device-relevant context, this review aims to provide a strategic and actionable perspective for advancing sustainable biochar-based supercapacitors beyond empirical optimization.

2. Biomass precursors and their composition

A high carbon content and favorable elemental composition (C, H, O, N) play a critical role in defining the structure, surface chemistry, and electrochemical behavior of biochar-based supercapacitor electrodes. To assess their suitability to produce biochar and energy storage applications, researchers have historically evaluated various lignocellulosic feedstocks, such as agricultural residues like rice husk, sugarcane bagasse, and rice husk, woody biomass such as hardwood, softwood, nut shells and organic wastes that includes biosolids and municipal organics [18–21]. Although most biomass feedstocks contain substantial fixed carbon suitable for electrode applications, their inherent ash and inorganic constituents particularly K, Na, Ca, and Mg, can significantly diminish the porosity and electrical conductivity of the resulting biochar if not properly removed. To meet electrode purity standards, water washing and mild acid leaching are commonly employed to eliminate soluble and acid-extractable metal impurities, thereby reducing ash content by over 90%. The porosity and conductivity of biochar can further be improved by chemical activation, making them suitable for high-performance supercapacitors applications [22–24]. Raw biomass preparation, particularly maintaining biomass moisture content below 10%, is essential in continuous pyrolysis systems to reduce drying related energy demand and increase operational safety. On the other hand, maintaining a volatile matter content in the range of 60–70% promotes effective pore formation, while simultaneously retaining enough fixed carbon to achieve desirable biochar yield [25].

2.1. Pyrolysis and carbonization pathways

Pyrolyzed biochar is a solid carbonaceous product obtained after the thermal decomposition of biomass, a process which involves heating a carbon-rich material under little oxygen or inert conditions. Among the various pyrolysis approaches, slow and fast pyrolysis are most utilized methods, with slow pyrolysis generally considered the most effective for its high biochar yield [26–28]. Slow pyrolysis is carried out at atmospheric pressure with moderate temperatures between 300 and 550°C, low heating rates between 0.1 and 0.8 °C min^{-1}, and extended residence times spanning from 5 to 30 min to as long as 25–35 h [29]. Slow pyrolysis is generally favored for biochar synthesis due to its longer residence time and controlled heating rate, which promotes higher solid yield (>30 wt percent), enhanced carbonization, and more stable pore structures, which is ideal for electrode applications. In contrast, fast pyrolysis biochar tends to be less ordered, more oxygen-rich, and obtained at lower yield lower (~10–20 wt%), which is less ideal for electrode fabrication. However, the rapid devolatilization can produce biochar's with greater specific surface areas (often >400 m^2/g) and well-developed pore structures. The pyrolysis temperature strongly influences biochar characteristics through volatile release, increasing temperature promotes further cracking of volatile fractions into low-molecular-weight gases and liquids rather than solid carbon, thereby reducing biochar yield [30–33]. Although the resultant porous structure can be beneficial for supercapacitor applications, the reduced solid yield remains a major limitation [21]. As summarized in Table 1, pyrolysis yields more stable, higher-mass biochar, while fast and flash processes favor volatile release and reduced char yield due to rapid heating.

2.2. Modification strategies for biochar electrochemical enhancement

The two principal, though occasionally overlapping, strategies for biochar modification in electrode applications are: (i) activation and

Table 1
Comparison of pyrolysis techniques for biochar production, highlighting operating conditions, yields, surface areas, and volatile release trends.

Pyrolysis	Temperature (°C)	Heating Rate(°C/s)	Biochar Yield(%)	BET Surface Area (m^2/g)	Volatile Matter Release	References
Slow	400–500	0.1–1	30–60	0.397 - 3.45(varied feedstocks)	VM ↓ as temp ↑	[34-36]
Fast	850–1250	10–200	15–30	Generally low	VM ↑	[34-36]
Intermediate	500–650	1.0–10	15–25	25 – 270 (varied stocks)	No data found	[37,38]
Vacuum	450–600	0.1–1.0	12	Not widely reported for biochar	Generally Lower than slow pyrolysis	[36,39]
Flash	900–1200	1000	30–50	< 20	No authentic data found	[34,36]

structural engineering, which improve porosity, surface area, and interfacial properties and are often extended through nanocomposite formation; and (ii) heteroatom doping, which tailors the electronic structure and surface chemistry by adding elements like N, S, P, or B into the carbon matrix. These approaches optimize the structural-interfacial and electronic-chemical domains of biochar, respectively, providing complementary ways of performance enhancement. In the subsequent sections, both modification approaches are discussed in detail, with emphasis on how they influence the structure–property relationships and overall capacitive behavior of biochar-based electrodes.

2.3. Activation and structural engineering

The pore structure and surface functionalities of biochar can be customized for supercapacitor applications through various physical and chemical activation techniques. Physical activation takes place at high temperatures, whereas chemical activation often includes low temperatures and lesser activation times than physical activation. Despite these benefits, chemical activation has certain downsides, including the necessity for post-activation water-washing to remove pollutants and the need for treatment facilities to handle polluted water. These reasons undermine the technique's environmental sustainability and cost-effectiveness [40]. In physical activation, pyrolysed biochar is exposed to oxidizing gases such as steam, CO_2, or air at 700–1100 °C. This selective oxidation of carbon atoms by steam or CO_2 generates micro- and mesoporous networks while preserving the carbon framework. Steam activation typically leads to higher carbon loss with abundant micropore formation, whereas CO_2 activation offers better control over pore development with reduced carbon loss [41]. The physical activation is valued for its environmental compatibility and scalability as it can yield surface areas of 700–900 m^2/g with specific capacitances around 90–100 F/g [21,42].

Chemical activation includes heating a biomass carbon precursor and activating agent to temperatures between 450 and 900 °C. Chemical activation has various benefits over physical activation, including lower pyrolysis temperatures, higher carbon yields, larger surface area (3600 m2 g^{-1}), and well-developed microporous structures [43]. In chemical activation, chemical compounds such as KOH, NaOH, or H_3PO_4 promote dehydration and redox reactions during pyrolysis, thereby enhancing pore formation and surface functionality. KOH activation is unique among chemical activation procedures, notably for increasing specific surface area and improving porous structure, which is beneficial for energy storage applications [44]. Compared to physical activation, chemical activation usually results in a significantly larger specific surface area (SSA) and microporosity. Within chemical activating agents, KOH is generally preferred, as acidic activators diminish conductivity, whereas KOH being the most reactive alkali yields superior porosity and electrochemical behavior. The porosity originates from the strong chemical interaction between KOH and the carbon matrix during activation, leading to the development of hierarchical structures [45]. As shown in Table 2, chemical activation using KOH or mixed KOH–H_3PO_4 yields the highest surface areas and tunable porosity, whereas physical agents like CO_2 and steam offer eco-friendly scalable activation routes.

2.3.1. Carbon-based composites

Carbon-based composites are designed to overcome the intrinsic energy-density limitation of pure biochar electrodes, which predominantly store charge through electric double-layer capacitance (EDLC) mechanisms [47]. While high surface area activated biochar can achieve capacitance values exceeding 300 F g^{-1} under optimized conditions, its energy density remains constrained by purely electrostatic charge storage.

The incorporation of redox-active components such as metal oxides, MXenes, or conductive polymers introduces faradaic charge storage pathways, enabling hybrid EDLC–pseudocapacitive behavior [48–53]. Structurally, the effectiveness of these composites depends on intimate interfacial contact between biochar and the active phase, hierarchical pore accessibility, and preservation of conductive carbon pathways.

For example, KOH/KNO_3-activated biochar derived from rose flower waste achieved a high specific surface area (~1980 m^2 g^{-1}) and delivered 350 F g^{-1} at 1 A g^{-1} in a three-electrode configuration [55]. The enhanced rate capability (165 F g^{-1} at 150 A g^{-1}) and long-term cycling stability (95.4% retention after 140,000 cycles) indicate that hierarchical porosity and conductive carbon backbone play a dominant role in sustaining pseudocapacitive enhancement. However, such high performance is strongly dependent on measurement configuration, as three-electrode systems may overestimate practical device-level metrics.

Metal oxide incorporation (e.g., RuO_2, MnO_2, NiO, Co_3O_4, V_2O_5) further increases theoretical capacitance through fast surface redox reactions [54]. Nevertheless, trade-offs frequently arise and volume expansion during cycling, interfacial resistance, and limited electrical conductivity can reduce rate performance and long-term durability. Consequently, composite performance is governed not solely by the intrinsic capacitance of the metal oxide phase but by the efficiency of charge transfer across the carbon-oxide interface and the stability of the composite architecture.

Cross-study discrepancies reported in composite performance commonly stem from differences in oxide loading fraction, particle dispersion, pore blocking effects, electrolyte type, and electrode mass loading. Excessive oxide incorporation may increase theoretical capacitance while simultaneously blocking micropores and reducing conductivity, thereby diminishing rate capability. Overall, carbon-based composites provide a pathway to enhanced energy density through

Table 2
Comparison of common activation methods for biochar-derived carbons, summarizing conditions, textural properties, yields, and key performance advantages.

Method	Temp (°C)	Agent Ratio	SSA (m^2/g)	Pore Volume	Yield	Key Advantages	Reference
CO_2	800	—	~800–1000	0.5–0.8	25–35	Clean, mild etching, scalable	[21,46]
Steam	750	—	1000–1400	0.6–1.0	20–30	Faster pore development, higher SSA	[39]
KOH	700–800	1:2–6:1	1500–2200	1.0–1.4	20–25	Very high SSA, tailored micro or meso pores	[42]
H_3PO_4 (or mixed KOH+H_3PO_4)	500–600	~1:1 or mixed	1500–1950	0.8–1.4	25–35	P-functional groups, pseudocapacitive enhancement	[46]

hybrid charge storage, but their practical effectiveness depends critically on interfacial engineering, oxide loading optimization, and preservation of conductive carbon networks.

2.3.1.1. Metal oxide–biochar composites. Metal oxide–biochar composites are designed to integrate the high electrical conductivity and structural stability of biochar with the redox-active properties of transition metal oxides such as MnO_2, Fe_3O_4, Co_3O_4, NiO, and layered double hydroxides (LDHs). In this hybrid architecture, biochar functions as a conductive scaffold that facilitates electron transport and prevents oxide particle agglomeration, while the metal oxide phase contributes faradaic pseudocapacitance through reversible surface or near-surface redox reactions [56–58].

Structurally, the effectiveness of these composites depends on homogeneous oxide dispersion, optimized oxide loading fraction, and preservation of hierarchical pore accessibility. Electrochemically, the introduction of metal oxides can substantially increase theoretical capacitance compared to pure biochar by adding redox-active sites beyond electric double-layer capacitance (EDLC). However, practical performance is strongly governed by interfacial charge transfer efficiency between the oxide phase and the carbon matrix.

Despite their enhanced redox activity, intrinsic limitations of metal oxides including low electrical conductivity and volume expansion during repeated cycling can compromise rate capability and long-term stability. Excessive oxide loading may block micropores, reduce accessible surface area, and increase internal resistance, thereby offsetting theoretical capacitance gains. Consequently, reported performance improvements vary widely across studies depending on oxide content, particle size distribution, electrolyte type, and electrode mass loading.

Cross-study discrepancies frequently arise from differences in synthesis method (hydrothermal vs. co-precipitation vs. in situ growth), oxide crystallinity, and carbon structural integrity. In systems where conductive pathways are preserved and oxide loading is carefully optimized, metal oxide-biochar composites achieve significant capacitance enhancement while maintaining acceptable cycling stability. Conversely, poorly engineered interfaces or high oxide fractions often lead to rapid performance decay. Overall, metal oxide-biochar composites represent a viable strategy for increasing energy density through hybrid charge storage, but their effectiveness relies on precise control of interfacial engineering, oxide dispersion, and structural integrity rather than simply maximizing redox-active content.

2.3.1.2. Polymer–biochar composites. Polymer-biochar composites are engineered to combine the high electrical conductivity and structural rigidity of biochar with the fast and reversible redox activity of conducting polymers such as polyaniline (PANI), polypyrrole (PPy), and poly(3,4-ethylenedioxythiophene) (PEDOT). Structurally, biochar functions as a mechanically robust and porous support matrix that suppresses polymer agglomeration, buffers volumetric expansion, and provide continuous conductive pathways for efficient electron transport [59–61].

Electrochemically, conducting polymers contribute substantial pseudocapacitance through reversible redox reactions occurring at heteroatom sites (e.g., amine/imine groups in PANI). These rapid ion–electron coupling processes significantly increase specific capacitance compared to EDLC-dominated carbon electrodes.

The hybrid architecture partially mitigates the degradation of biochar that restricts excessive polymer expansion and improves interfacial electron transfer, thereby enhancing cycling stability relative to pristine polymers. Nevertheless, performance variability across reported systems arises from differences in polymer loading fraction, polymer distribution within the pore network, electrolyte type, and electrode mass loading. Excessive polymer content can block micropores and reduce effective ion diffusion, while insufficient loading limits pseudocapacitive contribution. Consequently, polymer-biochar composite performance reflects a trade-off between redox-enhanced capacitance and mechanical durability. Optimal systems maintain moderate polymer content, uniform interfacial contact, and preserved pore accessibility to balance capacitance enhancement with long-term stability. Despite their high conductivity and flexibility, polymer swelling and contraction remain critical limiting factors for extended cycle life [59–61].

2.3.1.3. Carbonaceous nano-hybrid composites. Carbonaceous nano-hybrid composites integrate biochar with highly conductive carbon nanomaterials such as carbon nanotubes (CNTs) and graphene to enhance electron transport pathways and structural integrity. Structurally, the incorporation of CNTs or graphene introduces a percolated conductive network within the biochar matrix, reducing internal resistance and improving charge transport efficiency [62–64].

From an electrochemical perspective, this enhanced conductivity facilitates rapid electron transfer during charge–discharge cycles, thereby improving power density and rate capability. The high intrinsic surface area and layered architecture of graphene-like carbon frameworks also promote electrolyte ion diffusion and enable efficient pseudocapacitive contributions when combined with redox-active components such as PANI. Consequently, carbonaceous nano-hybrids frequently exhibit superior high-rate performance and enhanced cycling stability compared to pristine biochar electrodes.

However, the performance gains of nano-hybrid systems are strongly dependent on uniform nanocarbon dispersion and interfacial compatibility. Poor dispersion of CNTs or graphene can result in agglomeration, reduced accessible surface area, and ineffective conductive pathways, limiting practical performance improvement. Additionally, excessive nanocarbon loading may obstruct micropores and hinder ion transport. Cross-study discrepancies arise from variations in nanocarbon loading fraction, dispersion technique (e.g., in situ growth versus physical mixing), degree of graphitization, and electrolyte selection. While nano-hybrids significantly enhance rate capability and power density, their large-scale implementation remains constrained by the high cost of CNTs and graphene, as well as challenges associated with reproducible dispersion.

Overall, carbonaceous nano-hybrid composites represent a strategy primarily aimed at conductivity enhancement, power density optimization and practical utility depends on achieving uniform conductive networks at minimal nanocarbon loading to balance performance improvement with economic feasibility.

2.3.1.4. Core–shell metal–carbon composites. Core–shell metal carbon composites are architecturally designed systems in which a redox-active metal or metal oxide core is encapsulated within a conductive carbon shell. Structurally, the carbon shell functions as a protective and conductive barrier, restricting direct electrolyte exposure of the active core while maintaining continuous electron transport pathways [65,66].

From an electrochemical standpoint, this configuration enhances charge storage through two primary mechanisms. First, the conductive shell reduces interfacial resistance and facilitates rapid electron transfer between the core and the external circuit. Second, physical confinement of the metal oxide core mitigates volume expansion during redox cycling, thereby preserving structural integrity and improving cycling stability. Compared to simple metal oxide–biochar composites, core–-shell architectures often exhibit improved retention due to reduced pulverization and suppressed dissolution of active species.

However, performance is highly sensitive to shell thickness, core–-shell interface quality, and uniformity of encapsulation. An excessively thick carbon shell may hinder ion diffusion and limit utilization of the active core, while an insufficient shell may fail to suppress structural degradation. Additionally, non-uniform core distribution or incomplete encapsulation can result in localized stress accumulation and accelerated capacity fading.

As summarized in Table 3, hybrid systems such as NiFe-LDH/Biochar

Table 3
Comparison of biochar-based composite electrodes for supercapacitors, highlighting feedstocks, synthesis routes, capacitance, and cycling performance.

Composite Type	Feedstock	Capacitance (F/g)	Cycling Retention	Synthesis Method	Reference
MnO_2/Biochar	Wood, Bagasse, Banana peel	200–345	80–92% after 5000 cycles	Hydrothermal, Solvothermal	[67]
Fe_3O_4/Biochar	Rice husk, Corncob	150–300	up to 5000 cycles	Co-precipitation, Hydrothermal	[24,68]
NiFe-LDH/Biochar	Rice husk, Coconut shell	300–450	85–90% after 8000 cycles	Hydrothermal	[69]
PANI/Biochar	Sugarcane bagasse, Rice husk	350–400	65–75% at high current	In-situ polymerization	[70-72]
PEDOT/Biochar	Brewery bagasse, Agricultural waste	300–350	> 90%	Electropolymerization	[73]
CNT/Biochar	Rice husk, Corn cob	350–420	80–85%	In-situ CNT growth	[74] [75]
Fe–C (core–shell)	Rice husk, Peanut shell	250–300	High stability	Pyrolysis of Fe-doped biochar	[76]
Co–C (core–shell)	Wood-based biochar, Cashew shell	280–310	Stable and high-rate capability	Co-pyrolysis	[77,78]

and PANI/Biochar demonstrate enhanced capacitance and retention, reflecting the broader principle that interfacial engineering governs long-term electrochemical stability. Cross-study discrepancies in reported performance frequently arise from differences in core loading fraction, crystallinity, shell conductivity, and synthesis method (e.g., in situ growth versus post-encapsulation). Precise control over shell thickness and uniform dispersion remains a critical barrier to scalable production.

Overall, core–shell metal carbon composites represent an advanced strategy focused on interfacial stabilization and confinement-controlled redox behavior. Their practical success depends on balancing conductive shell thickness with ion accessibility to maximize active-site utilization while maintaining structural durability.

2.4. Heteroatom-doping

Heteroatom doping introduces external atoms into the carbon matrix of biochar, thereby altering its ion-accessible porosity, electronic distribution, and surface chemistry. This modification is typically categorized into metal-ion doping and non-metal element doping. While metal-ion doping is predominantly employed in anode materials to enhance electrical conductivity and charge transport, non-metal doping is more common in cathode materials due to its ability to introduce surface functionalities and active sites. In some cases, dual doping is employed, which involves the simultaneous incorporation of metal and non-metal species to synergistically enhance electrochemical performance. Along with creating adequate pore shapes, doping heteroatoms in the carbon structure is a typical technique for improving the electrochemical characteristics of porous carbon materials. This includes nitrogen [79,80], sulfur [81,82], phosphorous [83] and boron [84]. The doped carbon structure with pores is gaining attention with a variety of heteroatom sources being exploited. These ecologically friendly organic substances are used not only as a dopant of nitrogen-, sulfur-, or co-doped heteroatoms [85,86], as well as a carbon precursor for producing heteroatom-doped carbon-based compounds [87–89]. In doped biochar, structural and electronic changes enhance charge transfer kinetics, surface redox activity, and electrolyte wettability, which collectively govern the electrochemical performance of supercapacitors [90,91]. Doped biochar electrodes are therefore known to demonstrate distinctly improved electronic and ionic properties compared to their undoped counterparts [92–94]. Fig. 2 depicts the heteroatom doped structures of biochar enhances charge storage capacity of electrodes. To date, heteroatom doping of biochar has primarily focused on nitrogen (N), sulfur (S), and phosphorus (P) either individually or in combination, each imparting distinct structural and electrochemical functionalities, discussed in the following sections.

2.4.1. Nitrogen doping

Nitrogen doping represents one of the most effective and scalable strategies for enhancing biochar-based supercapacitor electrodes due to its simultaneous modulation of electronic structure and surface chemistry [95–99]. Nitrogen atoms are typically incorporated as pyridinic-N (N-6), pyrrolic-N (N-5), and graphitic-N (N-Q), with each configuration exerting distinct electrochemical effects. Pyridinic and pyrrolic nitrogen introduce defect sites and localized lone-pair electrons that promote surface redox reactions, whereas graphitic nitrogen enhances electrical conductivity through substitution within the carbon lattice [95–97].

From a structural perspective, the distribution and relative content of nitrogen species depend strongly on precursor chemistry and carbonization temperature, which govern both defect density and

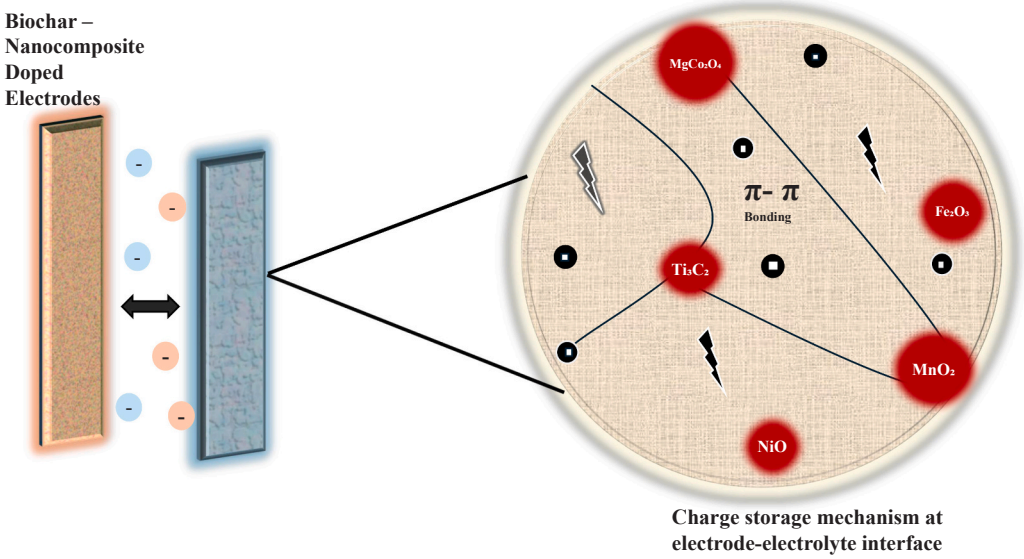

Fig. 1. Conceptual illustration of charge storage pathways within biochar–nanocomposite doped electrodes.

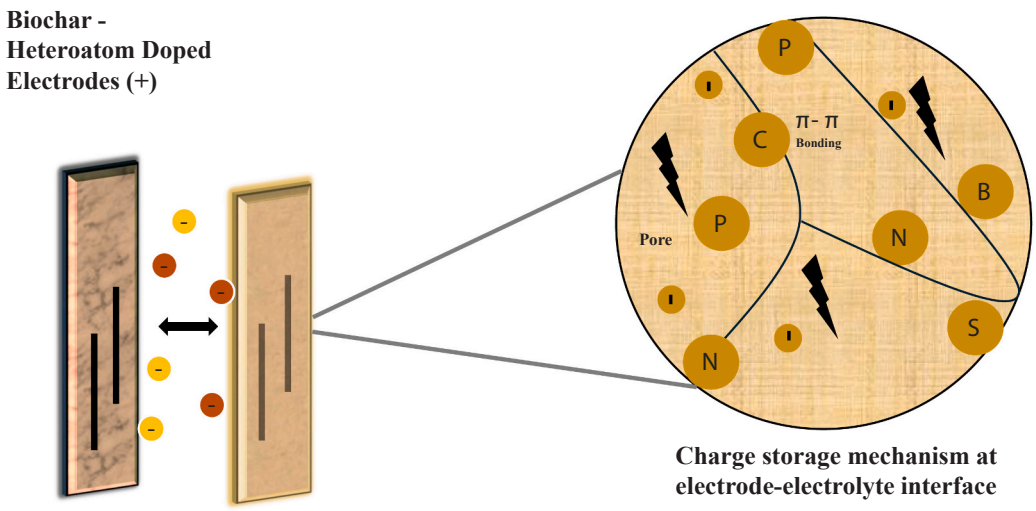

Fig. 2. Conceptual illustration of charge storage pathways within biochar– heteroatom doped electrodes.

graphitization degree [95,98]. Increased pyridinic-N content generally correlates with enhanced pseudocapacitive behavior, while excessive defect generation may disrupt conductive pathways and compromise rate capability [96–99].

Electrochemically, optimized nitrogen doping enhances electrolyte wettability and facilitates ion-accessible active sites, leading to improved charge storage kinetics. Several high-performance systems illustrate this structural-electrochemical synergy. For example, nitrogen-functionalized microporous carbon nanoparticles achieved approximately 391 F g^{-1} at 0.1 A g^{-1} in 6 M KOH, attributed to the combined effect of high specific surface area (~1938 m^2 g^{-1}) and nitrogen-enriched defect sites [138]. Similarly, activated nitrogen-doped carbons derived from biomass precursors demonstrated capacitance values up to ~385 F g^{-1} under alkaline conditions when hierarchical porosity was coupled with optimized nitrogen incorporation [139]. In contrast, systems with moderate nitrogen content and predominantly microporous structures more commonly report capacitance values in the range of 200–300 F g^{-1} [95–99], indicating that dopant concentration alone does not dictate performance.

Cross-study discrepancies in reported capacitance frequently arise from variations in electrolyte type (e.g., concentrated alkaline vs. neutral aqueous systems), electrode mass loading, and measurement configuration (two-electrode versus three-electrode testing), with the latter often yielding inflated capacitance values [95–99,138,139]. Furthermore, excessive nitrogen incorporation or aggressive activation may increase defect density but reduce graphitic conductivity, leading to diminished rate capability and cycling stability [96–99]. Overall, the collective evidence indicates that optimal nitrogen doping is achieved through a balanced interplay between defect-induced pseudocapacitance and preserved electronic conductivity, rather than maximization of total nitrogen content. Controlled dopant speciation combined with hierarchical pore architecture consistently yields the most favorable configuration between specific capacitance, rate capability, and long-term stability [95–99,138,139].

2.4.2. *Sulfur doping*

Sulfur doping modifies the carbon framework of biochar through the incorporation of thiophenic, sulfonic, and sulfide species, typically introduced via sulfur-containing precursors such as thiourea, elemental sulfur, Na_2S, or organosulfur compounds during pyrolysis, or by post-treatment sulfur vapor exposure [100–102]. Structurally, sulfur atoms introduce lattice distortion due to their larger atomic radius compared to carbon, altering local electronic density and potentially generating redox-active surface functionalities.

From an electrochemical perspective, sulfur-containing functional groups can enhance surface wettability and introduce additional pseudocapacitive reactions, contributing to improved charge storage kinetics [103–106]. In highly conductive carbon architectures such as sulfur-doped graphene and porous carbon nanosheets, capacitance values exceeding 300 F g^{-1} have been reported [107,108]. However, these systems typically benefit from inherently high conductivity and well-developed mesoporosity, which amplify the electrochemical contribution of sulfur functionalities.

In contrast, sulfur doping applied to activated carbon frameworks with limited structural optimization yields more modest performance enhancement. For example, the incorporation of 2.7% sulfur into activated carbon increased specific capacitance from 44.6 to 62.0 F g^{-1} at 1.4 A g^{-1} , representing a ~40% improvement but remaining substantially lower than graphene-based analogues [109]. This discrepancy highlights that sulfur incorporation alone does not guarantee high capacitance; rather, its electrochemical effectiveness is strongly dependent on the underlying pore architecture, electrical conductivity, and dopant distribution.

Several challenges remain associated with sulfur-doped biochar systems, including sluggish redox kinetics, limited rate capability, cycling degradation, and relatively low achievable energy density [110]. Excessive sulfur incorporation may also introduce structural instability or block micropores, reducing ion accessibility. Furthermore, cross-study variability arises from differences in sulfur content, precursor chemistry, porosity development, and electrolyte selection, making direct comparison of reported capacitance values difficult [100–102]. Collectively available evidence suggests that sulfur doping is most effective when integrated with hierarchical pore engineering and conductive carbon frameworks, rather than as a standalone modification strategy. Optimized sulfur content combined with controlled porosity can provide incremental capacitance enhancement, but the overall performance remains strongly governed by structural factors.

2.4.3. *Phosphorus doping*

Phosphorus doping in biochar exploits its multiple valence states and larger atomic radius, enabling out-of-plane substitution within the carbon lattice and inducing local structural distortion. During pyrolysis, phosphorus-containing functional groups such as C–P–O, C–O–P, P = O, and PO_3 are generated through interactions between phosphorus precursors and oxygen-containing surface sites. The formation and relative abundance of these groups are strongly governed by pyrolysis temperature and precursor chemistry [111].

From a structural perspective, phosphorus incorporation introduces

defect sites and modifies local charge density distribution, which can enhance surface polarity and electrolyte affinity. Electrochemically, these effects may promote additional redox-active sites and improve ion-accessible surface area. However, unlike nitrogen doping, phosphorus incorporation often reduces graphitization degree, thereby decreasing intrinsic electrical conductivity if not carefully controlled. The net electrochemical performance of phosphorus-doped biochar therefore reflects a balance between defect-induced pseudocapacitance and conductivity loss. Moderate phosphorus incorporation can enhance capacitance through increased surface functionality and improved electrolyte wettability, whereas excessive phosphorus content may disrupt conductive pathways and limit rate capability [111]. In systems where pore architecture and graphitic domains are preserved, phosphorus doping contributes to measurable capacitance enhancement; however, when graphitization is significantly suppressed, performance gains may plateau or decline.

Discrepancies in reported phosphorus-doped biochar performance frequently arise from variations in dopant concentration, pyrolysis temperature, precursor type, and pore development. Additionally, differences in electrolyte composition and electrode configuration complicate direct cross-study comparison. Consequently, phosphorus doping is most effective when integrated with controlled thermal treatment or co-doping strategies that preserve electronic conductivity while leveraging phosphorus-induced surface reactivity. Optimized phosphorus content combined with structural engineering is essential to achieve simultaneous improvement in capacitance, rate capability, and cycling stability.

2.4.4. Multi-element co-doping

As single-element doping approaches performance saturation, increasing attention has shifted toward multi-element co-doping strategies in biochar systems. Co-doping leverages synergistic interactions between heteroatoms such as N–B, N–S, or N–P combinations to engineer the carbon matrix in a more complex and tunable manner. Structurally, the simultaneous incorporation of multiple heteroatoms modifies lattice distortion, defect density, and charge redistribution beyond what is achievable through single-element substitution [112–115].

From an electronic perspective, co-doping can create complementary effects: for example, nitrogen introduces electron-rich defect sites, while boron acts as an electron acceptor, promoting localized charge polarization. The formation of C–N–B bonding configurations in N–B co-doped biochar has been shown to suppress the generation of polycyclic aromatic hydrocarbons (PAHs) during pyrolysis while stabilizing the carbon framework [116]. Such interactions highlight the broader structural impact of co-doping beyond simple additive effects of individual dopants.

Electrochemically, co-doping can enhance active site density, improve surface polarity, and promote synergistic pseudocapacitive behavior. However, the electrochemical response of co-doped systems is not always predictable. Emergent properties arise from dopant–dopant interactions, making performance outcomes highly sensitive to dopant ratio, spatial distribution, and thermal treatment conditions. Improper co-doping may increase structural disorder excessively, reduce electrical conductivity, or introduce unstable surface groups, thereby negatively affecting rate capability and cycling durability. To move beyond qualitative interpretation, quantitative assessment of co-doping synergy is essential.

Experimentally, synergy can be assessed by comparing the measured performance of co-doped systems against the weighted average performance of individually doped counterparts under identical testing conditions. A synergistic interaction may be inferred when the observed capacitance or energy density exceeds the linear combination predicted from single-element doping contributions.

From a modeling perspective, machine learning offers a systematic approach to quantifying interaction effects. Interaction terms between dopant concentrations can be explicitly incorporated into regression models, while tree-based ensemble methods inherently capture nonlinear feature interactions. Feature importance ranking and SHAP-based interaction analysis can further quantify whether combined dopant descriptors contribute more significantly than individual elements alone. However, current literature does not establish a universal composition window for optimal atomic ratios, as the effective ratio depends strongly on feedstock type, pyrolysis temperature, activation conditions, and electrolyte environment. Furthermore, performance landscapes often exhibit non-monotonic dependence on dopant ratios, suggesting the existence of system-specific optimal ranges.

Discrepancies in reported performance of co-doped biochar systems frequently stem from differences in dopant concentration ratios, precursor compatibility, porosity evolution, and graphitization degree. Moreover, the lack of standardized reporting on dopant speciation and bonding configuration complicates cross-study outcome comparison. Unlike single-element doping, where structure–property relationships are relatively well-established, co-doping introduces higher-dimensional design space complexity that challenges both experimental optimization and predictive modeling [111]. Overall, co-doping represents a promising but intrinsically complex approach demanding systematic experimental datasets utilization in conjunction with computational modeling to identify optimal dopant combinations and concentration windows that maximize output without sacrificing rate performance.

2.5. Approaches for heteroatom doping

2.5.1. In-situ doping

In situ, self-doping (endogenous) is achieved by directly carbonizing biowaste rich in the target element, enabling efficient heteroatom incorporation and consequent alteration of the biochar's surface area, functional groups, crystallinity, carbon defect density and active sites [117]. Heteroatoms like N, P, S and O can self-dope into biochar via pyrolysis, hydrothermal, or microwave processing. For example, the N and O in bamboo are retained during carbonization, enhancing pore formation in the resulting biochar [118]. This happens because nitrogen and oxygen species drive gas evolution and generate microchannels during devolatilization, which improves porosity while also providing surface-active areas conducive to redox reactions. In situ doping can also be achieved by combining biomass with external dopant sources such as phosphoric acid for P or urea for N, either prior to or during heat treatment. Such co-doping routes allow finer control over heteroatom concentration but may also cause competitive reactions between external and intrinsic species, influencing final dopant bonding configurations (e.g., pyridinic-N vs. graphitic-N, or C–O–P linkages). Chen et al. [119] reported successful synthesis of N-doped biochar from bamboo by pyrolyzing under an ammonia atmosphere [119]. Although self-doping is simple and low cost, accurately determining the type, quantity, and distribution of dopant within inherent material remains challenging [111].

2.5.2. Ex-situ doping

Biowastes with inherently low heteroatom content such as bagasse, maize stalks, grapefruit peels, fruit hulls, or banyan residues are exogenously (ex situ) doped by introducing external dopant as a post-treatment to achieve targeted heteroatom incorporation. Compared with in-situ doping, exogenous doping offers greater control over dopant concentration and distribution, as well as providing easier quantification of heteroatom levels in the resulting biochar [111]. Direct contact approaches and chemical vapor deposition (CVD) are the two main methods of exogenous doping. The CVD method offers excellent control over dopant uniformity and concentration, enabling precise incorporation of heteroatoms onto biochar surfaces via gas-phase reactions. In contrast, direct contact methods rely on physical mixing or impregnation of biochar with dopant precursors followed by thermal treatment.

Although simpler and more cost-effective, direct contact methods often lead to less uniform doping and weaker dopant–carbon bonding compared with CVD [120]. Wu et al. (2025) prepared N, O, and P co-doped biochar from sawdust using phosphoric acid and urea activation under air plasma post-treatment, achieving a surface area of 1240 m^2 g^{-1} , capacitance of 332 F g^{-1} at 1 A g^{-1} , and 94% retention after 5000 cycles [121]. Compared to in-situ methods, post-treatment doping often shows reduced efficiency and poor electrochemical stability owing to insufficient dopant anchoring [21]. The selection of appropriate biomass, doping method, and dopant level is critical for achieving biochar properties suited to the target application [111].

2.6. Physicochemical properties of modified biochar

2.6.1. Specific storage area and porosity

A high surface area and hierarchical pore structure are crucial for maximizing the electrode-electrolyte interface, facilitating ion diffusion, and enabling rapid charge accumulation. Nanocomposite modification often results in a substantial increase in SSA and total pore volume. This is mainly because nanoparticles inhibit pore collapse during carbonization and introduce additional mesopores. For instance, Ghori et al. [122] observed nearly an eight-fold rise in SSA (from 14 to 117 m^2 g^{-1}) when biochar was composited with $KCuCl_3$ nanoparticles. Other studies report even higher SSA (>2900 m^2 g^{-1}) creating a hierarchical pore network favorable for both ion transport and electrolyte penetration [122]. However, obtaining consistently dispersed hierarchical pores remains difficult, since uncontrolled nanoparticle aggregation or unequal activation can result in dead holes and decreased volumetric energy density. Thus, synthesis control and pore-size distribution optimization are critical for translating structural advantages into practical device performance. These structural gains translate into higher capacitance and rate capability [123]. GCN-S-0.5, a graphene–silk fibroin nanocomposite activated with KOH, delivered a specific capacitance of ~256 F g^{-1} at 0.5 A g^{-1} , the nanocomposite retained ~73.4% of capacitance at an ultrahigh current density of 50 A g^{-1} and maintained ~96.3% capacitance after 10,000 cycles, demonstrating both high-rate capability and excellent cycling stability [124].

Heteroatom doping, especially with nitrogen or phosphorus, can also enhance porosity through simultaneous activation. For example, co-activation using alkali salts (KOH and NaOH) and urea produces doped biochars exceeding 2200 m^2 g^{-1} [120]. In such systems, N and P containing precursors act both as dopants and activating agents, forming micro to mesoporous structures with abundant surface defects that contribute to redox-active sites. However, excessive activation can over-etch the carbon skeleton, jeopardizing mechanical integrity and electrical continuity. Balancing activation intensity and dopant concentration is consequently critical for maintaining conductivity while increasing accessible surface area. However, the porosity enhancement from doping is typically less pronounced compared to nanoparticle composites [125,126]. In summary, nanocomposite dominates in boosting physical pore architecture, while heteroatom doping refines surface chemistry and defect porosity, with both improving ion-accessible surface area but through distinct mechanisms.

2.6.2. Electrical conductivity

Electrical conductivity determines the charge transfer speed and influences both power density and cyclic stability. In heteroatom-doped biochars, conductivity arises from electronic structure modification. Nitrogen and phosphorus introduce defects that expand π-electron delocalization, lower the band gap, and enhance charge-carrier mobility [127]. These dopant-induced states act as charge hopping sites, allowing for quicker electron transport across sp^2 domains while maintaining the mechanical stiffness of the carbon framework. However, excessive dopant incorporation can result in scattering centers that impair overall mobility, emphasizing the importance of regulated doping concentration. Ehsani et al. [128] demonstrated that nitrogen doping can significantly enhance the electrical conductivity of biochar, boosting its electrochemical performance [128].

In contrast, nanocomposite biochar improve conductivity through electron pathways supported by conductive fillers such as rGO, Fe_3O_4, or transition metal oxides. These materials provide interconnected networks that bridge poorly conducting carbon domains, thereby minimizing internal resistance and accelerating redox kinetics [129]. Conducting polymers often undergo structural degradation, while metal oxides are constrained by limited electrical conductivity. Furthermore, repetitive volumetric expansion and contraction of metal oxides or conducting polymers during cycling can disturb interfacial connections, resulting in increased resistance and performance degradation. Strategies that combine flexible carbon scaffolds with nanoscale confinement of these materials assist in reducing deterioration. In contrast, self-co-doped heteroatom biochar provides a stable, highly conductive, and electrochemically efficient framework for advanced supercapacitor applications [130–132]. Thus, while doping supports intrinsic conductivity at the atomic scale, nanocomposites improve extrinsic pathways through percolation and interfacial properties. This multi-scale conduction synergy is a critical development for next-generation high--power supercapacitors.

2.6.3. Structural and morphological stability

Supercapacitors demand materials that retain structure under repeated charge–discharge cycles. Pure biochar, though lightweight and porous, tends to suffer from pore collapse and fragmentation upon cycling. Nanocomposite modification addresses this by introducing reinforcing nanostructures (Fe_3O_4, $CoFe_2O_4$, MnO_2) that act as mechanical stabilizers. These nanostructures serve not only as reinforcements, but also as stress distributors, turning localized strain into elastic deformation across the carbon matrix. Core–shell structures such as $CoFeO_4$@C maintain pore structure and resist aggregation during operation [133]. These structural frameworks distribute stress and preserve electrochemical integrity over long-term cycling. Heterogeneous particle loading can cause local stress spots and speed up deterioration, emphasizing the need for synthesis control in scalable electrode production. In electrochemical energy storage, nanocomposite-modified biochars retain their structure more effectively, resulting in longer service life and steadier performance [134]. On the other hand, heteroatom doping alters morphology by inducing microcracks and wrinkled textures through activation and gas release [120]. While this roughness enhances ion accessibility, excessive doping, especially with phosphorus at high temperature can degrade stability by over-etching or introducing weak crosslinking sites [135]. Controlled crack creation, on the other hand, can be helpful because it creates microchannels that allow for ion transport and electrolyte penetration. Hybrid techniques, which combine mild doping with nanostructural reinforcement, provide a feasible solution to improve ion transport while also increasing mechanical endurance.

2.7. Synergistic coupling of heteroatom doping and nanocomposite engineering

Recent developments increasingly combine heteroatom doping with nanocomposite engineering to achieve multi-scale optimization of biochar-based supercapacitor electrodes. While these two strategies are often discussed independently, their concurrent implementation can produce synergistic effects that exceed the performance enhancement achievable through either approach alone. The intrinsic synergy arises from the coupling of electronic modulation, interfacial charge transfer, and structural confinement within a unified architecture.

Heteroatom doping alters the electronic structure of the carbon matrix by introducing defect sites, modifying local charge density, and enhancing surface polarity. When nanocomposite phases such as MnO_2 are incorporated into doped carbon matrices, dopant-induced defects frequently act as anchoring and nucleation sites that promote uniform

oxide dispersion and stronger interfacial coupling. For example, MnO_2 integrated with sulfur-doped porous carbon spheres demonstrated improved packing density and electrochemical performance compared to undoped counterparts [49]. Similarly, MnO_2/nitrogen-doped graphene nanocomposites have shown enhanced charge transfer characteristics attributed to defect-mediated interfacial bonding and reduced internal resistance [54].

From a structural perspective, nanocomposite integration can compensate for certain limitations introduced by doping alone. Although high dopant concentrations may disrupt graphitic domains and reduce intrinsic conductivity, incorporation of redox-active phases such as MnO_2 can amplify pseudocapacitive contribution while the carbon matrix buffers volume expansion during cycling. In such dual-modified systems, the interplay between defect chemistry and heterojunction formation enables simultaneous enhancement of capacitance, rate capability, and cycling durability beyond singly modified systems.

The synergistic mechanism can therefore be interpreted as co-optimization of three coupled domains that includes electronic tuning through heteroatom-induced defect engineering, redox amplification via composite phase integration, and structural stabilization through hierarchical pore confinement. However, non-uniform dopant distribution or excessive composite loading may result in pore blockage, conductivity loss, or increased internal resistance. Unlike conventional reviews that treat doping and composite engineering as parallel modification routes, this integrated perspective highlights their co-engineering potential as a unified design paradigm. By intentionally coupling electronic and structural optimization, dual-modification strategies represent a critical pathway toward overcoming the inherent trade-offs of single-strategy approaches and advancing biochar-based supercapacitors toward higher energy density and operational stability. The multi-parameter interdependence inherent in such systems further expands the design space complexity, underscoring the necessity of data-driven and machine learning frameworks capable of navigating coupled structural-electronic electrochemical variables.

3. Performance comparison of biochar modification strategies in supercapacitors

The electrochemical performance of biochar-based supercapacitors is primarily governed by their specific surface area (SSA), porosity, electrical conductivity, and structural stability. Each of these properties influences the capacitance, energy density, and cycling stability of electrodes in distinct ways, while the modification route either nanocomposite formation or heteroatom doping lays the foundation.

3.1. Capacitance enhancement

Nanocomposites enhance charge storage primarily by increasing surface accessibility and introducing additional charge storage mechanisms. Guardia et al. [136] reported that composites of microporous carbon derived from grape seeds with reduced graphene oxide (rGO) achieved 260 F g^{-1} at 1 mA cm^{-2}, demonstrating that combining biochar with conductive nanomaterials can substantially improve electron transport and ion accessibility [136]. Shang et al. [137] developed nanocomposites from chitin nanofibers followed by carbonization to achieve a specific capacity of 128.5 F g^{-1} at 0.2 A g^{-1} [137]. In contrast, heteroatom doping enhances capacitance through the creation of additional active sites and pseudocapacitive behavior. Nitrogen doping (pyridinic, pyrrolic, and graphitic N) improves conductivity and introduces fast redox-active sites, while sulfur doping widens interlayer spacing and provides thiophenic redox centers. N, S co-doped biochar from pea peels achieved capacity of 80.25 F g^{-1} at 1 A g^{-1} , significantly higher than undoped carbon. Boron-doped biochar has been reported to have capacitance as high as 539.5 F g^{-1} , owing to strong surface polarization effects [95]. In another research, N-MCN was synthesized in a single-step reaction involving terephthalaldehyde and m-phenylenediamine in dioxane utilizing acetic acid as its catalyst. As-prepared N-MCNs assemble Qualities include a high surface area (~1938 m2 g), unusual porosity, distinctive shape, and nitrogen functional groups. The N-MCN850 electrode exhibits superb capacitive activity (391 F g at 0.1 A g), ultrahigh-rate effectiveness (145 F g at 100 A g), and persistent cycling stability (98% retention over 5000 cycles at 2 A g) in a 6 M KOH aqueous electrolyte. N-MCNs, with their superior efficiency, offer new options for supercapacitor applications [138]. Similarly, the weight ratio of NaOH/biochar majorly impacts carbon porosity and surface chemical composition. Specific surface area and nitrogen content can vary from 323 to 3012 m2 g−1 and 0.88–9.26 at%, respectively. Carbon's peculiar microstructure and nitrogen capabilities allow for a high capacitance of up to 385 F g^{-1} in 6 mol L^{-1} KOH aqueous electrolytes. This is due to the interaction of double layer capacitance and pseudo-capacitance. It has high rate potential (235 F g^{-1} at 50 A g^{-1}) and cycle endurance, which make it a viable substance for electrodes for supercapacitors as shown by Xu et al. (2012) [139]. While nanocomposites generally improve capacitance by facilitating charge transport and increasing surface area, heteroatom doping introduces chemical and electrochemical active sites that contribute pseudocapacitance. Nanocomposites often show higher absolute capacitance when paired with conductive additives like rGO, whereas heteroatom-doped biochars excel in boosting charge storage via redox reactions.

3.2. Energy density

Commercial supercapacitors typically utilize electrodes composed of pure carbon, which store charge primarily via the electrochemical double-layer mechanism. While this provides high power capability, the energy density of such devices is often low, limiting their application range [140]. For example, a supercapacitor with pure carbon electrodes was reported to have a maximum energy density of 0.762 Wh kg^{-1} at a power density of 184 W kg^{-1} [141]. Energy density ($E = \frac{1}{2}CV^2$) depends on both the specific capacitance (C) and the operating voltage (V). Nanocomposite electrodes improve energy density primarily through enhanced charge storage and ion transport via hierarchical porosity and conductive networks. Heteroatom-doped biochars, on the other hand, introduce pseudocapacitive sites and hydrophilic groups, which improve ion accessibility and translate into higher energy density at the device level. While dopants primarily enhance capacitance, they also improve electrode–electrolyte interactions, allowing safe operation at wider voltage windows in certain electrolytes [135]. Phosphorus and nitrogen co-doping also enhance meso-porosity and hydrophilicity, further boosting energy density by facilitating ion transport and redox reactions. Boron-doped biochar has been reported to attain an energy density of 40.5 Wh kg^{-1} , while N, S co-doped biochar reached 13.87 Wh kg^{-1} , both outperforming undoped biochar [135,142]. The relative advantage depends on the target application, nanocomposites excel when electron transport dominates, while heteroatom doping is more beneficial when redox-active sites contribute significantly to energy storage.

3.3. Cycling stability

For practical supercapacitor applications, cycling stability and capacitance retention are critical performance metrics. Nanocomposite electrodes can provide enhanced cycling stability by combining conductive networks with electroactive materials. The synergistic incorporation decreases volumetric strain and avoids active material separation during redox cycling, which is a frequent destruction route in single-phase electrodes. Furthermore, the conductive framework assures homogeneous current dispersion, minimizing localized excess potentials that generally boost failure. Zhao et al. [143] synthesized a porous Mn_2O_3/C@Co_3O_4 composite via a two-step hydrothermal process,

achieving a reversible specific capacitance of 523.8 F g^{-1} with 90.6% retention after 3000 cycles [143]. Similarly, nickel and manganese-based hybrid composite (NiO/MnO_2/BHC) demonstrated an 88% capacitance retention over 5000 cycles across a 1.6 V operating window [144]. These results highlight that well-designed composites can maintain high performance under extended cycling through stabilized electrode structure and electron transport facilitation. But the equilibrium of such nanocomposites frequently relies on interfacial connection force and lattice connectivity between phases. Weak coupling or imbalance can result into microcracking or interfacial resistance anticipation during extended cycling. Heteroatom-doped carbons, on the other hand, offer a distinct advantage in durability and long-term stability. Moderate doping reinforces the carbon framework and preserves conductive networks, mitigating capacitance degradation during repeated cycling. N-doped carbons typically retain 94–99% of their capacitance over 5000–10,000 cycles, while P-doped carbons have shown nearly 98% retention after 10,000 cycles [135]. Even co-doped systems (N, S or N, P) maintain $>$ 95% retention, demonstrating that carefully tuned doping not only enhances electrochemical performance but also ensures excellent durability for practical applications. Parameters such as carbonization temperature strongly influences hard carbon interlayer spacing and graphitization, which in turn also affects long-term stability [145]. Nanocomposites excel in stabilizing structure under cycling and facilitate rapid charge or discharge due to conductive additives and hierarchical porosity. While Heteroatom-doped biochars provide exceptional intrinsic durability, with doping reinforcing the carbon matrix and maintaining long-term capacitance retention. Selecting the appropriate strategy depends on the balance between absolute capacitance and long-term cycling stability.

3.4. Cost analysis

Heteroatom doping (N, P, S, B) on biomass carbons can remain near activated-carbon economics when using inexpensive dopants or activators like urea, melamine, H_3PO_4 or self-doped N-rich feedstocks. The price benefit enables heteroatom doping, especially appealing for large-scale deployment, as it depends on plentiful intermediate and simple manufacturing techniques. Furthermore, doping operations often take place under comparable thermal activation settings as traditional carbonization, necessitating no major capital modifications to current commercial setup. The estimated AC production costs cluster around \$2.7-\$2.9 kg^{-1} , with energy or activation the key OPEX driver [69,146]. The consumption of energy during activation frequently leads to operational expenses, particularly for chemical activators that require post-treatment or neutralization. Process intensification using microwave or hydrothermal activation has been proposed to cut consumption of energy by 30–40%, however industrial adoption is still restricted owing to scale-up and reactor design issues. Nanocomposite doping is price sensitive. MnO_2/NiO methods are consistently stated as low-cost/industrial-feasible, but graphene oxide drives costs dramatically upward \$400-\$700 kg^{-1} industrial and rGO \$50-\$150 kg^{-1} [147], [148]. Doped biochar is the most cost-effective option for commercial-size supercapacitors, but nanocomposite techniques have greater potential for high-performance specific uses.

As summarized in Table 4, biochar modification strategies demonstrate distinct and quantifiable trade-offs between electrochemical performance, durability, and techno-economic feasibility. Among the evaluated approaches, heteroatom-doped biochars currently represent the most industrially translatable strategy, combining high cycling stability (94–99%), competitive capacitance values ($>$200 F g^{-1}), and scalability enabled by low-cost precursors and single-phase structural modification. In contrast, metal oxide and polymer-based composites often achieve higher peak capacitance through faradaic contributions, yet suffer from interfacial degradation, volumetric expansion, and mechanical fatigue, which constrain long-term reliability and scale-up

Table 4
Integrated Comparative Framework of Biochar Modification Strategies for Supercapacitor Design.

Strategy	Dominant Mechanism	Typical Capacitance (F g^{-1})	Energy Density (Wh kg^{-1})	Cycling Stability (%)	Cost Level	Scalability	ML Predictability	Technology Maturity	Key Limitation	References
Physical Activation	Micropore-driven EDLC	90–150	$<$ 10	$>$ 90	Low	High	High (simple structural descriptors)	Commercially mature	Limited pseudocapacitance contribution	[21], [42]
Chemical Activation (KOH)	Hierarchical porosity + defect engineering	150–385	10–20	90–98	Medium	Medium	Moderate	Industrially feasible	Requires post-treatment; chemical waste handling	[43], [139]
Heteroatom Doping (N, S, P, B)	Electronic structure tuning + surface redox activity	200–500 +	10–40	94–99	Low–Medium	High	High (clear descriptors: SSA, ID/IG, dopant %)	Scalable academic–industrial bridge	Dopant instability or over-etching at high loading	[95], [135], [142]
Metal Oxide–Biochar Composites	Faradaic redox coupling	250–520	15–35	85–92	Medium	Medium	Moderate (multi-variable interfaces)	Academic-dominant	Volume expansion and conductivity decay	[143], [56]
Polymer–Biochar Hybrids	Surface redox polymer activity	200–400	10–25	80–90	Medium	Medium	Low–Moderate	Academic	Polymer swelling and mechanical fatigue	[59], [61]
Carbon Nano-Hybrid (rGO/CNT)	Conductive percolation network	250–420	15–30	90–95	High	Low	Moderate	Lab-scale	High material cost and aggregation challenges	[136], [62]
Core–Shell Metal–Carbon	Interfacial stabilization and confined redox	250–520	up to ~40	88–95	Medium–High	Low	Low–Moderate	Early-stage	Complex synthesis and shell thickness control	[76], [143]

potential. Carbon nano-hybrid systems enhance conductivity and rate capability; however, material cost and dispersion control make their adoption challenging. This integrated comparison provides a rational basis for strategy selection aligned with performance targets, cost constraints, and data-driven optimization objectives.

3.5. Overlaps and the case for integrated ML frameworks

Despite extensive studies on activation techniques, heteroatom doping, nanocomposite engineering, and the growing significance of machine learning in biochar-based supercapacitors independently, a unified perspective integrating these approaches remains lacking. The intrinsic overlaps between structural and electronic tuning are particularly critical for achieving synergistic optimization of conductivity, porosity, and electrochemical stability in biochar-based electrodes. For example, aggressive KOH activation facilitates in-situ incorporation of nitrogen or oxygen groups from the precursor or environment in addition to creating hierarchical porosity [149]. Such heteroatom doping, especially nitrogen or sulfur, can alter graphitization and pore distribution, which in turn affects textural properties [150]. Recognizing these overlaps avoids oversimplified distinctions and underscores the importance of unified design approaches for advancing biochar-based supercapacitors. The goal is to resolve these nonlinear interdependencies by employing approaches such as machine learning in bridging framework that links structural, electronic, and electrochemical descriptors. Our proposal for a multi-domain, physics-informed machine learning paradigm that incorporates textural, chemical, and electrochemical descriptors into interpretable models offers a logical path forward from compartmentalized datasets. A unique addition to the logical design of next-generation, sustainable supercapacitor materials are made by this viewpoint, which not only eliminates experimental redundancy but also makes predictive, closed-loop optimization of biochar electrodes possible. Fig. 3 illustrates the sequence of framework's data collection, designing models, and validation approaches for supercapacitor features prediction by ML models.

3.6. Mechanism-informed feature engineering and model interpretability

Most existing ML models in biochar-based supercapacitor research rely primarily on experimentally reported descriptors such as surface area, pore volume, and dopant concentration. However, deeper integration of physicochemical mechanisms requires customized feature engineering that encodes intrinsic electronic and structural behaviors. For example, π–π interactions between graphitic domains may be approximated using graphitization indices such as Raman ID/IG ratio, interlayer spacing metrics, or estimated aromatic cluster size derived from structural characterization. Charge redistribution associated with doped heteroatoms can be represented using XPS-derived bonding configurations (e.g., pyridinic-N, graphitic-N fractions) or electronegativity-weighted dopant descriptors. Similarly, pore evolution kinetics during activation may be parameterized using activation temperature gradients, heating rates, or micropore-to-mesopore ratios as proxies for diffusion-controlled pore development.

To quantify the contribution of these physically motivated descriptors, interpretability-driven validation strategies should be implemented. Feature analysis where mechanism-derived variables are selectively removed, can evaluate their incremental effect on cross-validated R^2 and mean absolute error. Explainable AI techniques such as SHAP (Shapley Additive Explanations) or permutation feature enable quantitative ranking of descriptor influence on predictive outputs [151, 152]. Improvements in extrapolation stability under constrained test sets or unseen synthesis conditions provide additional evidence of physically meaningful generalization. By systematically comparing empirical-only descriptor sets with mechanism-augmented feature spaces, the added value of physicochemical encoding can be quantitatively assessed. This approach enables ML frameworks to transition from statistical fitting toward physically grounded predictive modeling for biochar-based supercapacitors.

Current machine learning (ML) applications in biochar-based supercapacitors largely focus on supervised regression for performance prediction using tree-based ensembles and neural networks. However, next-generation progress requires integrated physics-data driven frameworks that embed electrochemical constraints directly into model architectures. Physics-informed machine learning (PIML), increasingly adopted in energy materials research [147–150], enables incorporation of physically meaningful descriptors such as defect density, effective electronic conductivity, ion diffusion length, and redox site density into predictive workflows.

An integrated framework can be structured into four coordinated layers. First, a standardized data architecture must harmonize structural descriptors (BET surface area, pore size distribution, Raman ID/IG ratio, dopant configuration), device-level parameters (mass loading, voltage window, electrolyte type), and durability metrics to improve cross-study generalizability [151]. Second, physics-informed constraints can be embedded via hybrid modeling approaches or regularization schemes that enforce thermodynamic consistency in predicted outputs, for example by constraining energy density predictions within voltage-dependent theoretical limits [152,153].

Third, multi-objective optimization should replace single-metric maximization. Practical implementation requires simultaneous optimization of capacitance, rate capability, cycling stability, mass loading, and cost. Pareto-front analysis and Bayesian optimization using Gaussian process regression provide systematic exploration of constrained design spaces while quantifying uncertainty [154,155]. Fourth,

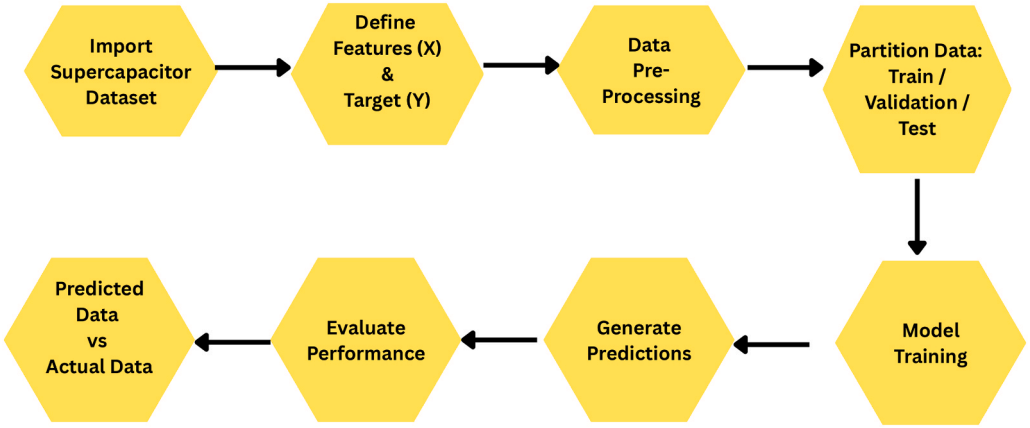

Fig. 3. Sequential workflow of the ML model from data acquisition to performance evaluation for supercapacitor property prediction.

closed-loop experimental workflows integrating active learning and uncertainty-guided sampling can iteratively recommend synthesis conditions, incorporate new experimental data, and retrain models to accelerate convergence in high-dimensional parameter spaces [156, 157].

By converging standardized data infrastructure, physics-informed modeling, multi-objective optimization, and adaptive experimentation, ML can evolve from correlation-driven prediction toward mechanistically guided and scalable materials design for biochar-based supercapacitors.

3.7. Application of advanced machine learning techniques

One of the most cutting-edge electrical energy storage technologies in recent years has been supercapacitors (SCs), which have the capacity to store up to 100 times more energy per unit volume/mass than traditional electrolytic capacitors [151,152]. SCs are often used in wearable technology, telecommunications, public transit, and the automobile industry. With advances in AI, data-driven materials research now enables precise prediction and rational design of novel materials with exceptional performance [153–155]. This synergy between AI and materials science heralds a new era of innovation in supercapacitor research, where intelligent data analysis enables the identification of promising materials and structural designs with the potential to transform energy storage technology. This interdisciplinary strategy will enhance the understanding of electrochemical processes and open new avenues for next-generation energy storage technologies.

3.8. Machine learning-guided investigation of nanocomposite and heteroatom doping in biochar-based supercapacitors

Nanocomposite biochar electrodes combine biochar conductivity with redox-active metal species to achieve synergistic charge storage behavior. Recent machine learning (ML) advances have systematically unraveled these nonlinear interdependencies, establishing quantitative links between synthesis variables and electrochemical performance [156]. Tang et al. [157] developed a comprehensive machine learning (ML) framework to predict the specific capacitance of $MgCo_2O_4$-based supercapacitor electrodes. Drawing upon literature-derived dataset comprising 324 experimental records, the study applied a hybrid recursive feature elimination (RFE) strategy to identify the most influential features controlling capacitance behavior. Among ML algorithms, Random Forest (RF), Extreme Gradient Boosting (XGBoost), and Regression Tree (RT), the XGB-RFE-XGB model (XGBoost serving as both selector and regressor) exhibited the highest predictive accuracy ($R^2 = 0.95$, RMSE $= 111.8$ F g^{-1}, and MAE $= 68.3$ F g^{-1}) [157].

Mulla et al. (2025) employed an XGBoost regression model trained on $NiCo_2S_4$/graphene datasets to quantitatively link synthesis variables to specific capacitance, achieving $R^2 \approx 0.95$ [158]. SHAP analysis revealed that 3D hierarchical and hollow nanostructures, balanced Ni/Co ratios, and optimal graphene content as the key determinants of electrochemical performance, highlighting ML's strength in resolving nonlinear structure–function relationships in bimetallic sulfide–carbon electrodes. Similarly, RF, SVR, GBR, XGBoost, and ANN models were employed to predict the specific capacitance of $NiCo_2O_4$/MXene composites, with XGBoost and ANN achieving the best performance ($R^2 \approx 0.96$). The optimal 20 wt% GNP composition delivered a specific capacitance of 226.6 F g^{-1} at 5 mV s^{-1} , with 84.2% retention after 5000 cycles. Mixed-phase NiO/Co_3O_4 composites typically trade gravimetric capacitance for enhanced rate capability and stability, a balance that ML techniques can effectively assess [159]. Three ML algorithms were developed and optimized including Bayesian Ridge Regression (BRR), K-Nearest Neighbors (KNN), and Artificial Neural Networks (ANN) for Ti_3C_2 MXene-based supercapacitors. The KNN model achieved the best performance ($R^2 = 0.928$, RMSE $= 0.040$), whereas the ANN model demonstrated capability to capture nonlinear interdependencies between input features. The study provided insights for establishing a scalable predictive route for supercapacitor design optimization [160].

Parwaiz et al. [161] applied machine-learning models to predict the cyclic-voltammetry (CV) of cobalt-based reduced graphene oxide nanocomposites, using scan-rate, potential, redox state and substitution level as input features [161]. Data-driven models including ANN and ensemble methods, were able to accurately map the complex electrochemical responses of composite electrodes, offering a rapid alternative to purely experimental CV characterization. Ravichandran et al. [162] used XGBoost, ANN, and RF models to predict current responses in cyclic voltammetry profiles of zinc and cobalt- substituted Bismuth ferrite ($BiFeO_3$) composites. All models achieved high predictive accuracy ($R^2 > 0.97$), demonstrating that ML can reliably forecast electrochemical behavior and specific capacitance directly from CV data, reducing experimental effort [162]. Overall, machine learning studies on nanocomposite biochar electrodes have demonstrated that tree-based ensemble (XGBoost, RF, GBR) and neural-network models (ANN) can effectively capture the nonlinear interdependence between metal type, loading ratio, and carbon support morphology. These approaches can accurately predict specific capacitance while revealing structure–function synergies, highlighting the potential of ML framework for identifying optimal design "sweet spots" in nanocomposite supercapacitors. Adding heteroatoms such as nitrogen (N), sulfur (S), phosphorus (P) or boron (B) to the sp^2 carbon lattice alters charge density and generates new surface functions, allowing for fast surface redox reactions [163], [164]. Recent studies have employed machine learning to identify structure-performance correlations in huge and diverse datasets of doped carbon materials. Mishra et al. [165] compiled a large database (~4899 experimental entries) of carbon electrodes, employed linear, support vector and tree-based models and showed that nonlinear models particularly XGBoost achieved superior predictive accuracy in capturing the complex interactions [165]. Furthermore, the study determined the most influential physicochemical descriptors for estimating specific capacitance and ranked them in priority order, identifying specific surface area and doping level as top ranked influencing descriptors. Similarly, Lu et al. [166] employed XGBoost, LightGBM, and deep neural networks to model the energy and power densities of biomass-derived carbon supercapacitors. Specific surface area, pore structure, and heteroatom content were identified as dominant descriptors governing performance whereas LightGBM achieved the best energy-density prediction ($R^2 = 0.922$) and XGBoost excelled in power-density prediction ($R^2 = 0.984$) [166].

Liao et al. [167] provided a deeper, more targeted mapping of structure-dopant performance relationships for a specific electrode material class, allowing optimization of descriptors rather than just ranking. Random Forest and XGBoost models using 303 literature entries were tested under uniform three-electrode conditions in 6 M KOH. The optimized XGBoost model with 5-fold cross-validation achieved $R^2 = 0.96$ and RMSE $= 15.83$, outperforming other regressors. SHAP interpretation revealed specific surface area and degree of graphitization as dominant descriptors. Among nitrogen functionalities, pyridinic-N (N-6) had the greatest positive effect and excess pyrrolic-N (N-5) suppresses performance. Partial-dependence analyses indicated optimal descriptor values yielding model-predicted maximum capacitance of ~303 F g^{-1} at 1 A g^{-1} [167]. On the contrary, Sun et al. [168] revealed that machine learning tools can quantitatively establish a correlation between biochar synthesis parameters such activation temperature and activation agent concentration to the resulting electrochemical capacitance, suggesting how initial preparation parameters influence performance [168]. For optimal performance, ML-guided analyses identified balanced ID/IG ratios that sustain electrical conductivity while retaining defect-active sites, moderate heteroatom doping levels and a meso-porosity range of 30–40% as the most favorable structural attribute [169]. In heteroatom-doped biochar systems, XGBoost, LightGBM, and RF models outperform linear regressors in resolving nonlinear couplings among dopant chemistry, porosity, and

graphitization degree, achieving $R^2 \approx 0.90–0.96$ across diverse datasets. SHAP interpretability has highlighted specific surface area, ID/IG ratio, and nitrogen speciation (notably pyridinic-N, N-6) as the most influential descriptors governing capacitance [170].

3.8.1. Strategy-specific models

Gradient boosting models have demonstrated high predictive fidelity for biomass-derived carbon systems, with LightGBM achieving $R^2 = 0.922$ for energy density and XGBoost reaching $R^2 = 0.984$ for power density. SHAP analysis further reveals that precursor composition and activation conditions act as dominant, system-specific determinants of electrochemical performance, reinforcing the importance of descriptor-level sensitivity in model construction [171]. Although ensemble models such as XGBoost and LightGBM often demonstrate strong predictive performance across aggregated datasets, the dominant governing factors for heteroatom-doped systems and nanocomposite-based systems differ fundamentally. Heteroatom doping primarily modulates electronic structure, defect chemistry, and surface polarity, whereas nanocomposite systems are additionally governed by interfacial heterojunction formation, phase dispersion, and structural stabilization effects. These distinctions imply divergence in descriptor distributions and feature relevance. A unified model trained on combined datasets may capture global correlations but risk underrepresenting subgroup-specific nonlinearities. Scenario-specific sub-models developed separately for heteroatom-doped and nanocomposite systems may improve interpretability and predictive robustness. Alternatively, hierarchical modeling approaches can be implemented, where an initial classifier distinguishes modification strategy type, followed by specialized regressors trained on strategy-relevant descriptors.

Comparative validation between unified and strategy-specific models can be assessed through cross-validation R^2, mean absolute error (MAE), and subgroup extrapolation stability. Statistically significant improvement in subgroup models would justify differentiated modeling architectures and reduce bias arising from descriptor heterogeneity. Such strategy-aware ML design offers a pathway toward more precise structure–performance mapping in biochar-based supercapacitors.

As summarized in Table 5, tree-based ensemble algorithms, particularly XGBoost and LightGBM, consistently outperform linear regressors across datasets ranging from approximately 300 to nearly 5000 entries. Predictive accuracy improves markedly when datasets are standardized by electrolyte condition and electrode configuration, as evidenced by higher R^2 values in curated subsets. Descriptor selection plays a decisive role in model robustness; specific surface area, dopant speciation, and graphitization degree repeatedly emerge as dominant features governing capacitance prediction. In contrast, multiphase composite systems introduce more complex and less constrained interfacial variables, which may limit cross-study model transferability [173]. These observations underscore the importance of structured feature reporting and standardized testing protocols for improving reproducibility and generalizability in ML-driven supercapacitor research.

4. Challenges and trends

Despite notable advances, several challenges continue to hinder the predictive reliability and transferability of ML models in biochar-based supercapacitor outcomes. In heteroatom-doped systems, data inconsistency and incomplete feature reporting remain major barriers such as many studies report only the total nitrogen content without resolving chemical states (pyridinic-, pyrrolic-, or graphitic-N) or merge data from two- and three-electrode configurations, resulting in model bias and limited generalizability. Similarly, nanocomposite datasets are often small, fragmented, and poorly annotated, with inconsistent descriptors for metal loading, dispersion, oxidation state, and carbon texture, which limits cross-study benchmarking and robust model training [172,174]. Bridging this gap requires data harmonization and hierarchical feature

Table 5
Summary of recent ML studies on supercapacitor performance prediction using carbon and biochar electrodes, highlighting dataset scope, model type, best algorithm, and reported performance metrics (R^2, RMSE, MAE).

Study Focus	Dataset Size	Target Variable	Key Input Features	Models Evaluated	Best Model	Best R^2	Additional Metrics	Validation Strategy	Reference
Carbon electrodes (EDLC)	4899 entries from 147 papers	Specific capacitance	SSA, pore volume, dopant level, electrolyte configuration	OLS, SVR, DT, RF, XGBoost	XGBoost	0.95*	Subset R^2: 0.89–0.95	Cross-validation	[165]
N-doped biochar (standardized 6 M KOH)	303	Specific capacitance	N-speciation, ID/IG ratio, SSA	RF, XGBoost	XGBoost	0.96	RMSE = 15.83	5-fold cross-validation	[149]
Biochar preparation–performance mapping	~300	Specific capacitance	Activation temperature, precursor type	RF, GBR, ETR	GBR	0.93	—	Cross-validation	[150]
Biomass-derived carbon electrodes	> 400	Energy density; Power density	Pore structure, heteroatom content	XGBoost, LightGBM, DNN	LGBM (energy); XGBoost (power)	0.922 (energy); 0.984 (power)	—	Cross-validation	[175]
Porous carbons (ML + experimental validation)	—	Specific capacitance	Textural and compositional descriptors	LR, RF, XGBoost, LGBM	LGBM	0.92	—	ML + experimental validation	[153]
$MgCo_2O_4$/carbon composites	324	Specific capacitance	Synthesis variables	9 hybrid RFE-based models	XGB-RFE-XGB	0.94	RMSE = 120 F g^{-1}; MAE = 62 F g^{-1}	RFE + cross-validation	[139]

integration across scales linking synthesis variables, microstructural features, and electrochemical metrics. Incorporating process-level descriptors (activation temperature, precursor type) with density function theory derived physicochemical properties such as adsorption energies and charge transfer at dopant sites can establish a mechanistic bridge between atomic-level electronic effects and device-level performance, providing a truly predictive basis for rational electrode design.

Recent methodological trends highlight a transition toward autonomous, data-centric experimentation powered by machine learning and closed-loop optimization. The integration of Bayesian optimization, active learning, and self-driving laboratory systems is revolutionizing materials discovery by replacing traditional "one-variable-at-a-time" experimentation with adaptive, feedback-driven synthesis workflows. These frameworks minimize failed synthesis attempts, reduce experimental costs, and accelerate the identification of optimal activation conditions, dopant ratios, and co-doping combinations for high-performance electrodes [175]. At the algorithmic frontier, physics-informed ML models such as graph neural networks (GNNs) and hybrid architectures incorporating pore-network descriptors, XPS-based heteroatom embeddings, and microscopy-derived morphological features are improving both prediction accuracy and interpretability. These models reveal how pore topology, ion mobility, and electronic structure co-govern charge storage behavior while maintaining generalizability across diverse feedstocks, electrolytes, and testing protocols [150]. The coupling of operando data streams with ML (e.g., in situ Raman or electrochemical impedance) is also emerging as a critical direction for capturing dynamic electrochemical processes in real time. Building on these achievements, inverse-design and generative ML models are now enabling the rational optimization of co-doped and nanocomposite biochar including tetra-element-doped carbons and ternary hybrids with transition-metal oxides, ferrites, or conducting polymers. These models facilitate balanced optimization of energy density, equivalent series resistance (ESR), cycle stability, and manufacturing cost under realistic synthesis constraints [176].

5. Conclusion and future perspective

Biochar-based supercapacitors represent a sustainable and structurally tunable platform that bridges circular biomass utilization with electrochemical energy storage. This review systematically evaluates heteroatom doping, nanocomposite engineering, and multi-element co-doping strategies within a unified structural electrochemical performance framework. The analysis demonstrates that performance enhancement in biochar systems arises from controlled defect engineering, electronic modulation, interfacial charge transfer optimization, and hierarchical pore architecture design. Heteroatom doping primarily improves electronic conductivity and surface redox activity, while nanocomposite integration amplifies pseudocapacitive contributions and structural stability. When co-engineered, these strategies offer synergistic pathways for enhancing capacitance, rate capability, and cycling durability. The incorporation of machine learning further shifts the field from empirical optimization toward predictive design, enabling identification of nonlinear structure–property relationships across synthesis variables and electrochemical metrics.

Despite these advances, several structural bottlenecks limit translation from laboratory demonstration to scalable deployment. In our assessment, the most immediate and impactful priority is the establishment of standardized data reporting and device-level benchmarking. Variability in electrolyte selection, voltage window, mass loading, electrode configuration (two- versus three-electrode systems), and normalization bases frequently obscures meaningful cross-study comparison. Without harmonized descriptors including dopant speciation, graphitization degree, pore size distribution, and conductivity metrics, machine learning models risk capturing dataset-specific correlations rather than transferable design principles. Addressing this issue requires community-level agreement on minimum reporting standards and consistent electrochemical testing protocols.

The second critical priority lies in realistic device-level validation. Many reported performance metrics are obtained under low mass loading (<2 mg cm^{-2}) or short cycling durations, conditions that do not reflect commercial supercapacitor operation. Future studies must emphasize practical electrode mass loading ($\geq$5–10 mg cm^{-2}), long-term cycling stability ($>$50,000 cycles), and performance retention under wide temperature ranges. Additionally, benchmarking against commercial activated carbon electrodes is essential to define genuine competitive advantages. Biochar systems must demonstrate not only enhanced gravimetric capacitance but also favorable cost-to-performance ratios, scalable synthesis routes, and environmental compatibility in activation processes. Green chemistry considerations, including reduced chemical waste in activation and sustainable precursor sourcing, remain essential for maintaining the ecological value proposition of biomass-derived materials.

From a data-driven perspective, progress depends on improved descriptor engineering and model interpretability. Physics-informed feature construction incorporating Raman ID/IG ratios, XPS-derived dopant bonding configurations, pore distribution metrics, and conductivity proxies can strengthen mechanistic alignment between structural parameters and predictive outputs. However, the feasibility of such approaches depends fundamentally on high-quality, standardized datasets. Multi-objective optimization frameworks, rather than single-metric maximization, represent a practical pathway forward. Real-world deployment requires simultaneous optimization of capacitance, rate performance, cycling stability, mass loading, and cost constraints. Techniques such as Pareto-front analysis and Bayesian optimization provide systematic tools for navigating these coupled trade-offs under realistic engineering boundaries.

High-impact, longer-term directions include the integration of hierarchical modeling architecture and closed-loop experimentation. Strategy-specific ML sub-models may better capture descriptor divergence between heteroatom-doped and nanocomposite systems, while active learning frameworks can iteratively refine synthesis conditions based on uncertainty-guided sampling. Although autonomous experimentation holds transformative potential, its widespread implementation remains limited by infrastructure cost and dataset scarcity. Therefore, incremental integration starting with uncertainty-aware model validation and constrained optimization is more feasible in the near term.

In multi-element co-doping systems, quantitative evaluation of dopant–dopant synergy remains an open challenge. Experimental comparison against weighted additive baselines, coupled with interaction-aware machine learning analysis, can clarify whether performance enhancement arises from genuine synergistic charge redistribution or from increased defect density alone. Current evidence suggests that optimal atomic ratios are system-dependent rather than universal, underscoring the importance of controlled parametric studies and compositional mapping.

Overall, the field is transitioning from isolated performance maximization towards integrated, reproducible, and constraint-aware design. The most impactful near-term investments should prioritize standardized electrochemical reporting and descriptor harmonization, realistic device-level validation under practical mass loading and cycling conditions, and interpretable, multi-objective ML modeling grounded in physicochemical principles. Longer-term efforts in closed-loop experimentation and multi-scale simulation offer substantial promise but require coordinated data infrastructure and collaborative frameworks.

CRediT authorship contribution statement

Rashid Iftikhar: Project administration, Investigation, Conceptualization. **Fatima Sajjad:** Writing – original draft, Methodology, Investigation. **Humayun Nadeem:** Writing – review & editing. **Sahar Saleem:** Writing – review & editing. **Alim-un-Nisa:** Writing – review & editing.

Salman Haider: Writing – review & editing. **Saifullah Zadran:** Writing – review & editing. **Muhammad Ali Inam:** Validation, Supervision.

Declaration of Generative AI and AI-assisted technologies in the writing process

During the preparation of this work the authors used Generative AI GPT 5 plus to rephrase. After using this tool, the authors reviewed the content as needed and take full responsibility for the content of the published article.

Declaration of Competing Interest

The authors declare that they have no known competing financial interests or personal relationships that could have appeared to influence the work reported in this paper.

Data availability

No data was used for the research described in the article.

References

[1] U. Safder, J. Loy-Benitez, C.K. Yoo, Techno-economic assessment of a novel integrated multigeneration system to synthesize e-methanol and green hydrogen in a carbon-neutral context, Energy 290 (Mar. 2024), https://doi.org/10.1016/j.energy.2023.130104.

[2] B.H. Cheng, R.J. Zeng, H. Jiang, Recent developments of post-modification of biochar for electrochemical energy storage, Elsevier Ltd, 2017, https://doi.org/10.1016/j.biortech.2017.07.060.

[3] H. J. and H.-Q.Y. Liu Wu-Jun, 'Emerging applications of biochar-based materials for energy storage and conversion ', *Energy Environ Sci*, vol. 12, no. 6, pp. 1751–1779, 2019, Accessed: Nov. 10, 2025. [Online]. Available: ⟨https://pubs.rsc.org/en/content/articlelanding/2019/ee/c9ee00206e⟩.

[4] A.M. Abioye, F.N. Ani, Recent development in the production of activated carbon electrodes from agricultural waste biomass for supercapacitors: A review, Elsevier Ltd, 2015, https://doi.org/10.1016/j.rser.2015.07.129.

[5] S. Rawal, B. Joshi, Y. Kumar, Synthesis and characterization of activated carbon from the biomass of Saccharum bengalense for electrochemical supercapacitors, J. Energy Storage 20 (Dec. 2018) 418–426, https://doi.org/10.1016/j.est.2018.10.009.

[6] A. Dutta, S. Mitra, M. Basak, T. Banerjee, A comprehensive review on batteries and supercapacitors: Development and challenges since their inception, John Wiley and Sons Inc, 2023, https://doi.org/10.1002/est2.339.

[7] M. Yu, Y. Peng, X. Wang, F. Ran, Emerging Design Strategies Toward Developing Next-Generation Implantable Batteries and Supercapacitors, John Wiley and Sons Inc, 2023, https://doi.org/10.1002/adfm.202301877.

[8] Weijia Zhou, Xiaojun Liu, Kai Zhou, Jin Jia, Carbon Materials for Supercapacitors, Nanomater. Adv. Batter. Supercapacitors (2016) 271–315.

[9] F. Bilgili, et al., The influence of biomass energy consumption on CO2 emissions: a wavelet coherence approach, Environ. Sci. Pollut. Res. 23 (19) (Oct. 2016) 19043–19061, https://doi.org/10.1007/s11356-016-7094-2.

[10] S. Wang, et al., Comparison of the pyrolysis behavior of lignins from different tree species, Biotechnol. Adv. 27 (5) (Sep. 2009) 562–567, https://doi.org/10.1016/j.biotechadv.2009.04.010.

[11] G.D.L.Z. Prof. S.W. Yingying Liu, 'Green Conversion of Microalgae into High-Performance Sponge-Like Nitrogen-Enriched Carbon', *Chem electro chem*, 2018.

[12] S. Wang, X. Guo, K. Wang, Z. Luo, Influence of the interaction of components on the pyrolysis behavior of biomass, J. Anal. Appl. Pyrolysis 91 (1) (2011) 183–189, https://doi.org/10.1016/j.jaap.2011.02.006.

[13] P.R. Yaashikaa, P.S. Kumar, S. Varjani, A. Saravanan, A critical review on the biochar production techniques, characterization, stability and applications for circular bioeconomy, Elsevier B.V, 2020, https://doi.org/10.1016/j.btre.2020.e00570.

[14] S.J. Johannes Lehmann, Biochar Environ. Manag. Sci. Technol. Implement. Taylor Fr. Group (2015), https://doi.org/10.4324/9780203762264.

[15] M.T.R.P.T.R.S.K.B.M.V.R.Y.S. Mitra Naghdi, Pine-wood derived nanobiochar for removal of carbamazepine from aqueous media: Adsorption behavior and influential parameters', Arab. J. Chem. (2019).

[16] L. Lonappan, et al., Adsorption of methylene blue on biochar microparticles derived from different waste materials, Waste Manag. 49 (Mar. 2016) 537–544, https://doi.org/10.1016/j.wasman.2016.01.015.

[17] M.N.S.K.B.E.J.K.M.V.A.A.R.R.Y.S.J.R.V.M. Taheran, 'Adsorption study of environmentally relevant concentrations of chlortetracycline on pinewood biochar', Sci. Total Environ. 571 (2016) 772–777.

[18] W. Chen, et al., Biomass pyrolysis for N-doped biochar: Relationship among preparation process. N-doped biochar properties, and supercapacitors, Elsevier Ltd, 2026, https://doi.org/10.1016/j.fuel.2025.136372.

[19] M. Jalali, Z. Panam, M. Jalali, W. Buss, The impact of feedstock type and pyrolysis parameters on the physical and chemical properties of biochars for sorption, agricultural and carbon sequestration applications: A meta-analysis, Elsevier B.V, 2025, https://doi.org/10.1016/j.jaap.2025.107271.

[20] M.K. Zafeer, R.A. Menezes, H. Venkatachalam, K.S. Bhat, Sugarcane bagasse-based biochar and its potential applications: a review, Inst. Ion. (2024), https://doi.org/10.1007/s42247-023-00603-y.

[21] R. Mehdi, A.H. Khoja, S.R. Naqvi, N. Gao, N.A.S. Amin, A Review on Production and Surface Modifications of Biochar Materials via Biomass Pyrolysis Process for Supercapacitor Applications, MDPI (2022), https://doi.org/10.3390/catal12070798.

[22] J. Zhou, X. Ren, Z. Liu, S. Yuan, Improving the cycling stability of biochar electrodes by purification via ion exchange, Mater. Today Sustain. 20 (Dec. 2022), https://doi.org/10.1016/j.mtsust.2022.100225.

[23] M. Ajorloo, M. Ghodrat, J. Scott, V. Strezov, Heavy metals removal/stabilization from municipal solid waste incineration fly ash: a review and recent trends, Springer, 2022, https://doi.org/10.1007/s10163-022-01459-w.

[24] Z. Song, T. Feng, D.W. Kirk, C.Q. Jia, Electrochemical Performance of Pre-Modified Birch Biochar Monolith Supercapacitors by Ferric Chloride and Ferric Citrate, Batteries 11 (2) (Feb. 2025), https://doi.org/10.3390/batteries11020047.

[25] N. Rambhatla, T.F. Panicker, R.K. Mishra, S.K. Manjeshwar, A. Sharma, Biomass pyrolysis for biochar production: Study of kinetics parameters and effect of temperature on biochar yield and its physicochemical properties, Results Eng. 25 (Mar. 2025), https://doi.org/10.1016/j.rineng.2024.103679.

[26] Y. Lee, P.R.B. Eum, C. Ryu, Y.K. Park, J.H. Jung, S. Hyun, Characteristics of biochar produced from slow pyrolysis of Geodae-Uksae 1, Bioresour. Technol. 130 (2013) 345–350, https://doi.org/10.1016/j.biortech.2012.12.012.

[27] M. Tripathi, J.N. Sahu, P. Ganesan, Effect of process parameters on production of biochar from biomass waste through pyrolysis: A review, Elsevier Ltd, 2016, https://doi.org/10.1016/j.rser.2015.10.122.

[28] P. Tanger, J.L. Field, C.E. Jahn, M.W. DeFoort, J.E. Leach, Biomass for thermochemical conversion: Targets and challenges, Frontiers Research Foundation, 2013, https://doi.org/10.3389/fpls.2013.00218.

[29] P. Roy, G. Dias, Prospects for pyrolysis technologies in the bioenergy sector: A review, Elsevier Ltd, 2017, https://doi.org/10.1016/j.rser.2017.03.136.

[30] S. Yu, J. Park, M. Kim, C. Ryu, J. Park, Characterization of biochar and byproducts from slow pyrolysis of hinoki cypress, Bioresour. Technol. Rep. 6 (Jun. 2019) 217–222, https://doi.org/10.1016/j.biteb.2019.03.009.

[31] M. Jouiad, N. Al-Nofeli, N. Khalifa, F. Benyettou, L.F. Yousef, Characteristics of slow pyrolysis biochars produced from rhodes grass and fronds of edible date palm, J. Anal. Appl. Pyrolysis 111 (Jan. 2015) 183–190, https://doi.org/10.1016/j.jaap.2014.10.024.

[32] F. Ronsse, S. van Hecke, D. Dickinson, W. Prins, Production and characterization of slow pyrolysis biochar: Influence of feedstock type and pyrolysis conditions, GCB Bioenergy 5 (2) (2013) 104–115, https://doi.org/10.1111/gcbb.12018.

[33] J. Park, Y. Lee, C. Ryu, Y.K. Park, Slow pyrolysis of rice straw: Analysis of products properties, carbon and energy yields, Bioresour. Technol. 155 (2014) 63–70, https://doi.org/10.1016/j.biortech.2013.12.084.

[34] M.K. Bahng, C. Mukarakate, D.J. Robichaud, M.R. Nimlos, Current technologies for analysis of biomass thermochemical processing: A review, Anal. Chim. Acta 651 (2) (Oct. 2009) 117–138, https://doi.org/10.1016/J.ACA.2009.08.016.

[35] L. Li, J.S. Rowbotham, H. Christopher Greenwell, P.W. Dyer, An Introduction to Pyrolysis and Catalytic Pyrolysis: Versatile Techniques for Biomass Conversion, N. Future Dev. Catal. Catal. Biomass-.-. Convers. (2013) 173–208, https://doi.org/10.1016/B978-0-444-53878-9.00009-6.

[36] L. Zhang, C. (Charles) Xu, P. Champagne, Overview of recent advances in thermochemical conversion of biomass, Energy Convers. Manag 51 (5) (May 2010) 969–982, https://doi.org/10.1016/J.ENCONMAN.2009.11.038.

[37] G. SriBala, H.H. Carstensen, K.M. Van Geem, G.B. Marin, Measuring biomass fast pyrolysis kinetics: State of the art, John Wiley and Sons Ltd, 2019, https://doi.org/10.1002/wene.326.

[38] A. Shaaban, S.M. Se, M.F. Dimin, J.M. Juoi, M.H. Mohd Husin, N.M.M. Mitan, Influence of heating temperature and holding time on biochars derived from rubber wood sawdust via slow pyrolysis, J. Anal. Appl. Pyrolysis 107 (May 2014) 31–39, https://doi.org/10.1016/J.JAAP.2014.01.021.

[39] E.T. Awoh, J. Kiplagat, S.K. Kimutai, A.C. Mecha, Sonication-assisted activation of empty fruit bunches to produce activated carbon for supercapacitor's electrodes: Surface chemistry and morphology characterization, Heliyon 10 (21) (Nov. 2024) e38975, https://doi.org/10.1016/J.HELIYON.2024.E38975.

[40] Ms.P.H. Dr.P.B.S.Ms Shilpa Simon, Green Power: The Role of Plant-Based Biochar in Advanced Energy Storage', ChemPhysChem (2024).

[41] E.T. Awoh, J. Kiplagat, S.K. Kimutai, A.C. Mecha, Sonication-assisted activation of empty fruit bunches to produce activated carbon for supercapacitor's electrodes: Surface chemistry and morphology characterization, Heliyon 10 (21) (Nov. 2024), https://doi.org/10.1016/j.heliyon.2024.e38975.

[42] J. Cheng, et al., Impact of Activation Conditions on the Electrochemical Performance of Rice Straw Biochar for Supercapacitor Electrodes, Molecules 30 (3) (Feb. 2025), https://doi.org/10.3390/molecules30030632.

[43] M. Galinski, K. Babeł, K. Jurewicz, Performance of an Electrochemical double layer capacitor based on coconut shell active material and ionic liquid as an electrolyte, J. Power Sources 228 (Apr. 2013) 83–88, https://doi.org/10.1016/J.JPOWSOUR.2012.11.048.

[44] Y.S. Yun, et al., Microporous carbon nanoplates from regenerated silk proteins for supercapacitors, Adv. Mater. 25 (14) (2013) 1993–1998.

[45] K. Jedynak, B. Charmas, Adsorption properties of biochars obtained by KOH activation, Adsorption 30 (2) (Feb. 2024) 167–183, https://doi.org/10.1007/s10450-023-00399-7.

[46] A. Pimsawat, A. Tangtrakarn, N. Pimsawat, A. Khamkongkaeo, S. Daengsakul, Microwave assisted activation of silkworm excrement for fast adsorption of methylene blue and high performance supercapacitor, Sci. Rep. 14 (1) (Dec. 2024), https://doi.org/10.1038/s41598-024-77568-3.

[47] S. Raviolo, et al., Valorization of brewer's spent grain via systematic study of KOH activation parameters and its potential application in energy storage, Biomass-.-. Bioenergy 192 (Jan. 2025), https://doi.org/10.1016/j.biombioe.2024.107494.

[48] a Y. B. a S. C. a Z. H. b P. W. a Y. Q and S.Z. Xiaoxiao Ma, 'A composite of pineapple leaf-derived porous carbon integrated with ZnCo-MOF for high-performance supercapacitors', *Physical Chemistry Chemical Physics*, no. 45, 2024.

[49] S. Yao, L. Chen, Y. Guo, S. Zong, H. Zhang, J. Feng, Hydrangea-like MnO2@sulfur-doped porous carbon spheres with high packing density for high-performance supercapacitor, J. Electroanal. Chem. 976 (Jan. 2025), https://doi.org/10.1016/j.jelechem.2024.118802.

[50] Y. Wang, et al., Hydrangea-like NiMn layered double hydroxide grown on biomass-derived porous carbon as a high-performance supercapacitor electrode, Ind. Crops Prod. 222 (Dec. 2024), https://doi.org/10.1016/j.indcrop.2024.120035.

[51] L. Wei, W. Deng, S. Li, Z. Wu, J. Cai, J. Luo, Sandwich-like chitosan porous carbon Spheres/MXene composite with high specific capacitance and rate performance for supercapacitors, J. Bioresour. Bioprod. 7 (1) (Feb. 2022) 63–72, https://doi.org/10.1016/j.jobab.2021.10.001.

[52] K.K.R. Reddygunta, B.D. Kumar, Biomass Activated Carbon Composites and Their Potential in Supercapacitor Applications: Current Trends and Future Perspectives, American Chemical Society, 2024, https://doi.org/10.1021/acs.energyfuels.4c01159.

[53] Suman, G. Rani, R. Ahlawat, H. Kumar, Green source-based carbon quantum dots, composites, and key factors for high-performance of supercapacitors, J. Power Sources 617 (Oct. 2024) 235170, https://doi.org/10.1016/J.JPOWSOUR.2024.235170.

[54] H.R. Naderi, P. Norouzi, M.R. Ganjali, Electrochemical study of a novel high performance supercapacitor based on MnO2/nitrogen-doped graphene nanocomposite, Appl. Surf. Sci. 366 (Mar. 2016) 552–560, https://doi.org/10.1016/J.APSUSC.2016.01.058.

[55] R.A.S. Dr, J.P. Prof, Y.S. Prof, X.L. Prof, Abrar Khan, Hierarchically Porous Biomass Carbon Derived from Natural Withered Rose Flowers as High-Performance Material for Advanced Supercapacitors', BATTERIES suppercaps (2020).

[56] Y.N. Zhang, C.Y. Su, J.L. Chen, W.H. Huang, R. Lou, Recent progress of transition metal-based biomass-derived carbon composites for supercapacitor, Springer, 2023, https://doi.org/10.1007/s12598-022-02142-7.

[57] X. Yang, T. Lv, J. Qiu, High Mass-Loading Biomass-Based Porous Carbon Electrodes for Supercapacitors: Review and Perspectives, John Wiley and Sons Inc, 2023, https://doi.org/10.1002/smll.202300336.

[58] N. Waris, et al., A Review on Development of Carbon-Based Nanomaterials for Energy Storage Devices: Opportunities and Challenges, American Chemical Society, 2023, https://doi.org/10.1021/acs.energyfuels.3c03213.

[59] M.F. Ahmer, Q. Ullah, M.K. Uddin, Magnetic metal oxide assisted conducting polymer nanocomposites as eco-friendly electrode materials for supercapacitor applications: A review, Walter de Gruyter GmbH, 2025, https://doi.org/10.1515/polyeng-2024-0101.

[60] D. Jiang, et al., Electromagnetic Interference Shielding Polymers and Nanocomposites - A Review', Apr. 03, Taylor Fr. Inc. (2019), https://doi.org/10.1080/15583724.2018.1546737.

[61] H.K. a, O. logo *a B. J. B. a R. S. O. logo a G. K. a R. K. a A. D. a A. Y. a D. S. O. logo b and P. K. Aarti Tundwal, 'Developments in conducting polymer-, metal oxide-, and carbon nanotube-based composite electrode materials for supercapacitors: a review, RSC Adv. 14 (2024).

[62] M. Zhong, M. Zhang, X. Li, Carbon nanomaterials and their composites for supercapacitors', Sep. 01, John Wiley Sons Inc. (2022), https://doi.org/10.1002/cey2.219.

[63] V.T. Nguyen, et al., Biomass-derived materials for energy storage and electrocatalysis: recent advances and future perspectives', Dec. 01, Springer, 2024, https://doi.org/10.1007/s42773-024-00388-1.

[64] H. He, et al., Functional Carbon from Nature: Biomass-Derived Carbon Materials and the Recent Progress of Their Applications', Jun. 02, John Wiley Sons Inc. (2023), https://doi.org/10.1002/advs.202205557.

[65] D. Liu, et al., Flexible Fiber-Shaped Supercapacitors: Structures, Materials, Fabrication Methods, and Applications', May 01, John Wiley Sons Inc. (2025), https://doi.org/10.1002/idm2.12243.

[66] S. Mourdikoudis, A. Kostopoulou, A.P. LaGrow, Magnetic Nanoparticle Composites: Synergistic Effects and Applications', Jun. 01, John Wiley Sons Inc. (2021), https://doi.org/10.1002/advs.202004951.

[67] F.Z. Kouidri, A.A. Alayyaf, M. Kiari, A. Benyoucef, B.D. Alkoudsi, L. Sabantina, Enhancing Supercapacitor Performance Using Co-doped Biochar Embedded on Oxide Metal/polyaniline Ternary Composite as Electrode Materials, J. Inorg. Organomet Polym. Mater. 35 (5) (May 2025) 3415–3427, https://doi.org/10.1007/s10904-024-03464-y.

[68] M.A. Abdallah, et al., Green Pomegranate Peel and Potato Peel Starch-Derived Magnetic Nanocomposite as Efficient Sorbent of Ascorbic Acid Extracted from Fruit Juices, Food Bioproc Tech. 18 (5) (May 2025) 4443–4460, https://doi.org/10.1007/s11947-024-03728-y.

[69] T. Zhang, J. Li, Mild and Efficient One-Step Synthesis of Nitrogen-Doped Multistage Porous Carbon for High-Performance Supercapacitors, Molecules 28 (24) (Dec. 2023), https://doi.org/10.3390/molecules28248136.

[70] M.R. Fornari, B.M. Hryniewicz, T.T.S. Matos, J. Schultz, M. Vidotti, A. S. Mangrich, Graphene-like biochars from pyrolysis of sugarcane bagasse and exhausted black acacia bark for the production of supercapacitors, Biomass-.-. Bioenergy 193 (Feb. 2025) 107567, https://doi.org/10.1016/J.BIOMBIOE.2024.107567.

[71] I. Radja, et al., Construction of a ternary composite of mg-doped biochar/CuO, and PAni for supercapacitor applications, J. Energy Storage 108 (Feb. 2025) 114785, https://doi.org/10.1016/J.EST.2024.114785.

[72] T. Yu, P. Zhang, L. Chen, L. Huang, H. Wu, X. Zhou, Preparation of high-performance supercapacitors using bark activated carbon/polyaniline composite electrode, Biomass-.-. Bioenergy 197 (Jun. 2025) 107813, https://doi.org/10.1016/J.BIOMBIOE.2025.107813.

[73] T.A. Hamdalla, S.A. Al-Ghamdi, S. Alfadhli, A.M. Alsharari, M. Chiesa, S. Khasim, PEDOT: PSS Doped Activated Biochar as a Novel Composite Material for Photocatalytic and Efficient Energy Storage Application, Catalysts 14 (9) (Sep. 2024), https://doi.org/10.3390/catal14090630.

[74] F. Mahmood, et al., A review of biochar production and its employment in synthesizing carbon-based materials for supercapacitors, Ind. Crops Prod. 227 (May 2025) 120830, https://doi.org/10.1016/J.INDCROP.2025.120830.

[75] D.C. M. A, N.T. Rishabh Anand Omar, Functional Nanoparticle-Coated Biochar (FNs-BC)-Based Composites and Their Applications, Compos Sci. Technol. (2025) 73–105.

[76] Y. Ye, et al., Core–shell structure carbon coated ferric oxide (Fe2O3@C) nanoparticles for supercapacitors with superior electrochemical performance, J. Alloy. Compd. 639 (Aug. 2015) 422–427, https://doi.org/10.1016/J.JALLCOM.2015.03.113.

[77] F. Wei, J. Jiang, G. Yu, Y. Sui, A novel cobalt–carbon composite for the electrochemical supercapacitor electrode material, Mater. Lett. 146 (May 2015) 20–22, https://doi.org/10.1016/J.MATLET.2015.01.143.

[78] A.J.B.R.B.R.R.N.R.T.A.H.R.R.K.Bandhana Devi, 'Cobalt-Embedded N-Doped Carbon Nanostructures for Oxygen Reduction and Supercapacitor Applications', ACS Appl. Nano Mater. 3 (7) (2020).

[79] G. Lin, R. Ma, Y. Zhou, Q. Liu, X. Dong, J. Wang, KOH activation of biomass-derived nitrogen-doped carbons for supercapacitor and electrocatalytic oxygen reduction, Electro Acta 261 (Jan. 2018) 49–57, https://doi.org/10.1016/j.electacta.2017.12.107.

[80] Yuanfu Deng, Ye Xie, Kaixiang Zoua, Xiulei Ji, Review on recent advances in nitrogen-doped carbons: preparations and applications in supercapacitors, J. Mater. Chem. A Mater. 4 (2016).

[81] S. Huo, et al., Methanesulfonic acid-assisted synthesis of N/S co-doped hierarchically porous carbon for high performance supercapacitors, J. Power Sources 387 (May 2018) 81–90, https://doi.org/10.1016/j.jpowsour.2018.03.061.

[82] H. Tang, D. Yan, T. Lu, L. Pan, Sulfur-doped carbon spheres with hierarchical micro/mesopores as anode materials for sodium-ion batteries, Electro Acta 241 (Jul. 2017) 63–72, https://doi.org/10.1016/j.electacta.2017.04.112.

[83] J. Yi, et al., Lignocellulose-derived porous phosphorus-doped carbon as advanced electrode for supercapacitors, J. Power Sources 351 (2017) 130–137, https://doi.org/10.1016/j.jpowsour.2017.03.036.

[84] Wang Xin, Lu Han, Yonghui Song, Jianfeng Peng, and Ruixia Liu, 'Synthesis of Biomass-Derived Mesoporous Carbon with Super Adsorption Performance by an Aqueous Cooperative Assemble Route', *ACS Sustainable Chemistry & EngineeringVol 5/Issue 3Article*, vol. 5, no. 3.

[85] G.P. Hao, W.C. Li, S. Wang, G.H. Wang, L. Qi, A.H. Lu, Lysine-assisted rapid synthesis of crack-free hierarchical carbon monoliths with a hexagonal array of mesopores, Carbon N. Y 49 (12) (Oct. 2011) 3762–3772, https://doi.org/10.1016/j.carbon.2011.05.010.

[86] Stephanie-Angelika Wohlgemuth, Filipe Vilela, Maria-Magdalena Titiricia, Markus Antoniettia, A one-pot hydrothermal synthesis of tunable dual heteroatom-doped carbon microspheres, Green. Chem. (2012).

[87] X. Gao, et al., Direct Heating Amino Acids with Silica: A Universal Solvent-Free Assembly Approach to Highly Nitrogen-Doped Mesoporous Carbon Materials, Adv. Funct. Mater. 26 (36) (Sep. 2016) 6649–6661, https://doi.org/10.1002/adfm.201601640.

[88] G. Ma, Z. Zhang, H. Peng, K. Sun, F. Ran, Z. Lei, Facile preparation of nitrogen-doped porous carbon for high performance symmetric supercapacitor, J. Solid State Electrochem. 20 (6) (Jun. 2016) 1613–1623, https://doi.org/10.1007/s10008-016-3171-1.

[89] M. Zhou, et al., A Molecular Foaming and Activation Strategy to Porous N-Doped Carbon Foams for Supercapacitors and CO2 Capture, Nanomicro Lett. 12 (1) (Feb. 2020), https://doi.org/10.1007/s40820-020-0389-3.

[90] R.L. Shrestha, et al., Nanoporous carbon materials derived fromwashnut seed with enhanced supercapacitance, Materials 13 (10) (May 2020), https://doi.org/10.3390/ma13102371.

[91] T.D.K.K.Y.K.H.K.T.A.K.N. George Hasegawa, 'High-Level Doping of Nitrogen, Phosphorus, and Sulfur into Activated Carbon Monoliths and Their Electrochemical Capacitances', Chem. Mater. 27 (13) (2015).

[92] Q. Liu, Z. Hu, C. Zou, H. Jin, S. Wang, L. Li, Structural engineering of electrode materials to boost high-performance sodium-ion batteries, Cell Rep. Phys. Sci. 2 (9) (Sep. 2021) 100551, https://doi.org/10.1016/J.XCRP.2021.100551.

[93] K.T.K.S.P.A. VAN A. Y. Y, J.M. Lijun Fu, 'Nitrogen doped porous carbon fibres as anode materials for sodium ion batteries with excellent rate performance', Nanoscale 3 (2014).

[94] X. Zhang, X. Cheng, Q. Zhang, Nanostructured energy materials for electrochemical energy conversion and storage: A review, J. Energy Chem. 25 (6) (Nov. 2016) 967–984, https://doi.org/10.1016/J.JECHEM.2016.11.003.

[95] M.A.H. A W. M, S.Y.P. G. G. N. L.-S, A.S. G. K, Wasiu Olakunle Makinde, 'Heteroatom co-doped green pea peel-derived biochar for high-performance energy storage applications', RSC Adv. 20 (2025).

[96] A. Kaur, O.P. Pandey, L.K. Brar, Synergic effect of B and N dopants in graphene for supercapacitance and electrochemical sensing applications, J. Phys. Chem. Solids 180 (Sep. 2023) 111460, https://doi.org/10.1016/J.JPCS.2023.111460.

[97] R. Liu, J.X. Wang, W.D. Yang, Hierarchical Porous Heteroatoms—Co-Doped Activated Carbon Synthesized from Coconut Shell and Its Application for Supercapacitors, Nanomaterials 12 (19) (Oct. 2022), https://doi.org/10.3390/nano12193504.

[98] S. Liu, et al., Nitrogen-Doped Porous Carbons Derived from Peanut Shells as Efficient Electrodes for High-Performance Supercapacitors, Int J. Mol. Sci. 25 (14) (Jul. 2024), https://doi.org/10.3390/ijms25147583.

[99] Y. Li, X. Xu, Y. He, Y. Jiang, K. Lin, Nitrogen doped macroporous carbon as electrode materials for high capacity of supercapacitor, Polym. (Basel) 9 (1) (2017), https://doi.org/10.3390/polym9010002.

[100] A.C.J.Z. B R. L, Q.L.C. Z. Y. B. Z.-H, H.W. S, F.K. Xiaoliang Yu, 'Facile synthesis of nitrogen-doped carbon nanosheets with hierarchical porosity for high performance supercapacitors and lithium–sulfur batteries', J. Mater. Chem. A Mater. 36 (2015).

[101] B. Karamanova, A. Stoyanova, M. Shipochka, C. Girginov, R. Stoyanova, On the cycling stability of biomass-derived carbons as electrodes in supercapacitors, J. Alloy. Compd. 803 (Sep. 2019) 882–890, https://doi.org/10.1016/J.JALLCOM.2019.06.334.

[102] Y. Deng, Y. Ji, H. Wu, F. Chen, Enhanced electrochemical performance and high voltage window for supercapacitor based on multi-heteroatom modified porous carbon materials, Chem. Commun. 55 (10) (2019) 1486–1489, https://doi.org/10.1039/C8CC08391F.

[103] A.Y.Z. B P. T. C, D.J. Cheng Zhan, 'Enhancing graphene capacitance by nitrogen: effects of doping configuration and concentration', Phys. Chem. Chem. Phys. 6 (2016).

[104] Q. Xu, G. Yang, X. Fan, W. Zheng, Improving the quantum capacitance of graphene-based supercapacitors by the doping and co-doping: first-principles calculations, ACS Omega 4 (8) (Aug. 2019) 13209–13217, https://doi.org/10.1021/acsomega.9b01359.

[105] P.A. Denis, R. Faccio, A.W. Mombru, Is it possible to dope single-walled carbon nanotubes and graphene with sulfur? ChemPhysChem 10 (4) (Mar. 2009) 715–722, https://doi.org/10.1002/cphc.200800592.

[106] W. Song, et al., Tuning the Double Layer of Graphene Oxide through Phosphorus Doping for Enhanced Supercapacitance, ACS Energy Lett. 2 (5) (May 2017) 1144–1149, https://doi.org/10.1021/acsenergylett.7b00275.

[107] A.M.O. A. B S. A. A, M.H. C, supercapacitor electrode materials Nazish Parveen, 'Simultaneous sulfur doping and exfoliation of graphene from graphite using an electrochemical method for supercapacitor electrode materials', JOURNALS Mater. Chem. A (1) (2016).

[108] A.Y.Z. A L, Y. A Y. T, A.M. M, Q.X. Wenfang Deng, 'Sulfur-doped porous carbon nanosheets as an advanced electrode material for supercapacitors', RSC Adv. 17 (2015).

[109] Y. Huang, et al., Sulfurized activated carbon for high energy density supercapacitors, J. Power Sources 252 (Apr. 2014) 90–97, https://doi.org/10.1016/J.JPOWSOUR.2013.12.004.

[110] X. Chen, et al., Emerging Nitrogen and Sulfur Co-doped Carbon Materials for Electrochemical Energy Storage and Conversion', Mar. 19, John Wiley Sons Inc. (2025), https://doi.org/10.1002/smll.202412191.

[111] J. Zhao, Y. Jiang, X. Chen, C. Wang, H. Nan, Unlocking the potential of element-doped biochar: from tailored synthesis to multifunctional applications in environment and energy', Dec. 01, Springer, 2025, https://doi.org/10.1007/s42773-025-00467-x.

[112] J. Zhao, Y. Li, Z. Xu, D. Wang, C. Ban, H. Zhang, Unique porous Mn2O3/C cube decorated by Co3O4 nanoparticle: Low-cost and high-performance electrode materials for asymmetric supercapacitors, Electro Acta 289 (Nov. 2018) 72–81, https://doi.org/10.1016/J.ELECTACTA.2018.09.042.

[113] Wu-Jun LiuOrcidWen-Wei, Li.Hong JiangOrcidHan-Qing, Yu Orcid, Fates of Chemical Elements in Biomass during Its Pyrolysis, Chem. Rev. 117 (9) (2017).

[114] Y. Liu, S. Yao, Y. Wang, H. Lu, S.K. Brar, S. Yang, Bio- and hydrochars from rice straw and pig manure: Inter-comparison, Bioresour. Technol. 235 (Jul. 2017) 332–337, https://doi.org/10.1016/J.BIORTECH.2017.03.103.

[115] Y. He, et al., Consequence of replacing nitrogen with carbon dioxide as atmosphere on suppressing the formation of polycyclic aromatic hydrocarbons in catalytic pyrolysis of sawdust, Bioresour. Technol. 297 (Feb. 2020) 122417, https://doi.org/10.1016/J.BIORTECH.2019.122417.

[116] C.M. Hung, C.W. Chen, C.P. Huang, Y.Y. Yang, C.Di Dong, Suppression of polycyclic aromatic hydrocarbon formation during pyrolytic production of lignin-based biochar via nitrogen and boron co-doping, Bioresour. Technol. 355 (Jul. 2022) 127246, https://doi.org/10.1016/J.BIORTECH.2022.127246.

[117] X. Zheng, et al., In-situ synthesis of NiS-modified MgO/S-doped biochar for boosting the adsorption-photocatalytic activity, J. Ind. Eng. Chem. 126 (Oct. 2023) 492–500, https://doi.org/10.1016/J.JIEC.2023.06.037.

[118] K. Chaturvedi, et al., Bamboo for producing charcoal and biochar for versatile applications', Jul. 01, Springe Sci. Bus. Media Dtschl. GmbH (2024), https://doi.org/10.1007/s13399-022-03715-3.

[119] W. F. Y, L.K. C. Z, X.M. G. M, C.Y. Y. H, T.X. C. H, Chen, 'Bamboo wastes catalytic pyrolysis with N-doped biochar catalyst for phenols products, in: Applied Energy, 260, Elsevier, 2020.

[120] N. Ahmed, et al., Advancements in Biochar Modification for Enhanced Phosphorus Utilization in Agriculture', May 01, Multidisciplinary Digital Publishing Institute (MDPI), 2024, https://doi.org/10.3390/land13050644.

[121] Zongjin Wu, et al., Sawdust-based N, O and P co-doped porous biochar for high-performance supercapacitors', N. J. Chem. (26) (2025).

[122] M.I. Ghori, et al., Harnessing biochar based metal halide (KCuCl3) for highly efficient energy storage application, J. Energy Storage 119 (May 2025) 116253, https://doi.org/10.1016/J.EST.2025.116253.

[123] Y. Geng, et al., Situ N, O-Dually Doped Nanoporous Biochar Derived from Waste Eutrophic Spirulina for High-Performance Supercapacitors, Nanomaterials 13 (17) (Sep. 2023), https://doi.org/10.3390/nano13172431.

[124] Y. Wang, Y. Song, Y. Wang, X. Chen, Y. Xia, Z. Shao, Graphene/silk fibroin based carbon nanocomposites for high performance supercapacitors, J. Mater. Chem. A Mater. 3 (2) (2015) 773–781, https://doi.org/10.1039/C4TA04772A.

[125] H. Yang, et al., Effect mechanism of phosphorous-containing additives on carbon structure evolution and biochar stability enhancement, Biochar 6 (1) (Dec. 2024), https://doi.org/10.1007/s42773-024-00330-5.

[126] S. Chen, L. Tian, X. Feng, H. Bao, H. Wang, Biomaterial-derived porous carbon doped with heteroatoms as a separator coating for high-energy–density Zn-I batteries, Biochar 6 (1) (Dec. 2024), https://doi.org/10.1007/s42773-024-00399-y.

[127] N. Kasera, P. Kolar, S.G. Hall, Nitrogen-doped biochars as adsorbents for mitigation of heavy metals and organics from water: a review', Dec. 01, Springer, 2022, https://doi.org/10.1007/s42773-022-00145-2.

[128] A. Ehsani, H. Parsimehr, Electrochemical energy storage electrodes from fruit biochar, Adv. Colloid Interface Sci. 284 (Oct. 2020) 102263, https://doi.org/10.1016/J.CIS.2020.102263.

[129] A. ATEŞ, K.O. OSKAY, Preparation and characterization of nanosized Fe3O4-biochar electrocatalysts with large surface area for H2O2 sensing, Surf. Interfaces 29 (Apr. 2022) 101733, https://doi.org/10.1016/J.SURFIN.2022.101733.

[130] G.A. Snook, P. Kao, A.S. Best, Conducting-polymer-based supercapacitor devices and electrodes, J. Power Sources 196 (1) (Jan. 2011) 1–12, https://doi.org/10.1016/J.JPOWSOUR.2010.06.084.

[131] J.M.C.L. Hao Jiang, Mesoporous Carbon Incorporated Metal Oxide Nanomaterials as Supercapacitor Electrodes', Adv. Mater. (2012).

[132] R.R. Salunkhe, Y.V. Kaneti, Y. Yamauchi, Metal-Organic Framework-Derived Nanoporous Metal Oxides toward Supercapacitor Applications: Progress and Prospects', Jun. 27, Am. Chem. Soc. (2017), https://doi.org/10.1021/acsnano.7b02796.

[133] M. Haghshenas, M. Mazloum-Ardakani, F. Tamaddon, A. Nasiri, CoFe2O4@methyl cellulose core-shell nanostructure and their hybrids with functionalized graphene aerogel for high performance asymmetric supercapacitor, Int J. Hydrog. Energy 46 (5) (Jan. 2021) 3984–3995, https://doi.org/10.1016/J.IJHYDENE.2020.10.253.

[134] M. Kaur, H. Kaur, Synergistic effect of biochar impregnated with ZnO nano-flowers for effective removal of organic pollutants from wastewater, Appl. Surf. Sci. Adv. 12 (Dec. 2022) 100339, https://doi.org/10.1016/J.APSADV.2022.100339.

[135] new journal of chemistry, 'Boron-doped biomass-derived nanocarbon for efficient supercapacitors: bridging waste recycling and energy storage', *Dharmender Singh Rana, Ritika Sharma, Abhishek Awasthi,d Dilbag Singh and Anshu Sharma*, no. 32, 2025.

[136] L. Guardia, et al., Biomass waste-carbon/reduced graphene oxide composite electrodes for enhanced supercapacitors, Electro Acta 298 (Mar. 2019) 910–917, https://doi.org/10.1016/J.ELECTACTA.2018.12.160.

[137] Z. Shang, et al., Chitin nanofibers as versatile bio-templates of zeolitic imidazolate frameworks for N-doped hierarchically porous carbon electrodes for supercapacitor, Carbohydr. Polym. 251 (Jan. 2021) 117107, https://doi.org/10.1016/J.CARBPOL.2020.117107.

[138] Y. Zhao, et al., Nitrogen-functionalized microporous carbon nanoparticles for high performance supercapacitor electrode, Electro Acta 153 (Jan. 2015) 448–455, https://doi.org/10.1016/J.ELECTACTA.2014.11.173.

[139] Bin Xu, Shanshan Hou, Feng Wu, Yusheng Yanga, Gaoping Cao, Sustainable nitrogen-doped porous carbon with high surface areas prepared from gelatin for supercapacitors, ' J. Mater. Chem. (36) (2012).

[140] Y. Jiang, C. Zhou, J. Liu, A non-polarity flexible asymmetric supercapacitor with nickel nanoparticle@ carbon nanotube three-dimensional network electrodes, Energy Storage Mater. 11 (Mar. 2018) 75–82, https://doi.org/10.1016/J.ENSM.2017.09.013.

[141] Z. Husain, et al., Nano-sized mesoporous biochar derived from biomass pyrolysis as electrochemical energy storage supercapacitor, Mater. Sci. Energy Technol. 5 (Jan. 2022) 99–109, https://doi.org/10.1016/J.MSET.2021.12.003.

[142] Y. Yang, Z. Shao, Boron and nitrogen co-doped carbon nanospheres for supercapacitor electrode with excellent specific capacitance, Nanotechnology 33 (18) (Apr. 2022), https://doi.org/10.1088/1361-6528/ac4eb2.

[143] J. Zhao, Y. Li, Z. Xu, D. Wang, C. Ban, H. Zhang, Unique porous Mn2O3/C cube decorated by Co3O4 nanoparticle: Low-cost and high-performance electrode materials for asymmetric supercapacitors, Electro Acta 289 (Nov. 2018) 72–81, https://doi.org/10.1016/J.ELECTACTA.2018.09.042.

[144] A.B.X.Z.B.X. Y. B X. Z, B.R. Meiqing Fan, 'Rational design of asymmetric supercapacitors via a hierarchical core–shell nanocomposite cathode and biochar anode', RSC Adv. 72 (2019).

[145] G. He, X. Yuan, Y. Wang, M. Yilmaz, J. Li, S. Yuan, N, S-codoped porous biochar derived from bagasse-based polycondensate for high-performance CO2 capture and supercapacitor, Sep Purif. Technol. 354 (Feb. 2025) 128826, https://doi.org/10.1016/J.SEPPUR.2024.128826.
[146] A.J.S.B.Z. W. A Z. Z, A.Y.Z. A Y. L, B. L. H, C.Y. Qiuli Chen, 'Sustainable rose multiflora derived nitrogen/oxygen-enriched micro-/mesoporous carbon as a low-cost competitive electrode towards high-performance electrochemical supercapacitors', RSC Adv. 17 (2018).
[147] B. Bounor, et al., Low-cost micro-supercapacitors using porous Ni/MnO2 entangled pillars and Na-based ionic liquids, Energy Storage Mater. 63 (Nov. 2023) 102986, https://doi.org/10.1016/J.ENSM.2023.102986.
[148] H. Soltani, H. Bahiraei, S. Ghasemi, M. Hashempour, Rate capability and electrolyte concentration: Tuning MnO2 supercapacitor electrodes through electrodeposition parameters, Heliyon 11 (1) (Jan. 2025) e41427, https://doi.org/10.1016/J.HELIYON.2024.E41427.
[149] W. Chen, et al., Biomass pyrolysis for N-doped biochar: Relationship among preparation process, N-doped biochar properties, and supercapacitors, Fuel 404 (Jan. 2026) 136372, https://doi.org/10.1016/J.FUEL.2025.136372.
[150] K.Y.L.Z.W.W.S. Z. B. W. M. X. S. Y, R.T. Xinhua Liu, A Fast Forward Prediction Framework for Energy Materials Design Based on Machine Learning Methods, Energy Mater. Adv. 5 (2024).
[151] R. Kötz, M. Carlen, Principles and applications of electrochemical capacitors, Electro Acta 45 (15–16) (May 2000) 2483–2498, https://doi.org/10.1016/S0013-4686(00)00354-6.
[152] H. Yuan, D. Tan, X. Wei, H. Dai, Fault Diagnosis of Fuel Cells by a Hybrid Deep Learning Network Fusing Characteristic Impedance, IEEE Trans. Transp. Electrification 10 (1) (Mar. 2024) 1482–1493, https://doi.org/10.1109/TTE.2023.3272654.
[153] J.W.P.P.W.J.S.S.T.T.L. D. P. S. J. S. J. R. S, A.C. Edward, O. Pyzer-Knapp, Accelerating materials discovery using artificial intelligence, high performance computing and robotics, NPJ Comput. Mater. 84 (8) (2022).
[154] D.W.D. H. C. O. I, A.W. Keith, T. Butler, Machine learning for molecular and materials science, Nature 559 (2018) 547–555.
[155] N.O. Lide, M. Rodriguez-Martinez, 'Emerging Nanotechnologies in Rechargeable Energy Storage Systems', 1, Elsevier, 2017.
[156] A.P. Khedulkar, V.D. Dang, A. Thamilselvan, R.A.N. Doong, B. Pandit, Sustainable high-energy supercapacitors: Metal oxide-agricultural waste biochar composites paving the way for a greener future, J. Energy Storage 77 (Jan. 2024) 109723, https://doi.org/10.1016/J.EST.2023.109723.
[157] M. Tang, Y. Ding, T. Hu, X. Zhu, G. Zheng, Y. Tian, Machine Learning-Based Prediction of Supercapacitor Capacitance for MgCo2O4 Electrodes, ChemPhysChem 25 (21) (Nov. 2024), https://doi.org/10.1002/cphc.202400629.
[158] H.S. Mulla, et al., Machine Learning a Predictive Tool for the Analysis of NiCo2S4/Graphene Composites for Supercapacitor', Jul. 17, John Wiley Sons Inc. (2025), https://doi.org/10.1002/cssc.202402559.
[159] M. Shariq, et al., Machine learning models for prediction of electrochemical properties in supercapacitor electrodes using MXene and graphene nanoplatelets, Chem. Eng. J. 484 (Mar. 2024) 149502, https://doi.org/10.1016/J.CEJ.2024.149502.
[160] Sanjith Krishna, Afkham Mir, Unlocking the potential of Ti3C2 electrodes: a data-driven capacitance prediction study', R. Soc. Chem. 3 (2024) 2986–2998.
[161] Shaikh ParwaizOwais Ahmed, MalikDebabrata PradhanMohammad, Mansoob Khan, Machine-Learning-Based Cyclic Voltammetry Behavior Model for Supercapacitance of Co-Doped Ceria/rGO Nanocomposite', J. Chem. Inf. Model 58 (12) (2018).
[162] Abhilash RavichandranValliappan, RamanYogapriya SelvarajPrabhavathy, MohanrajHemalatha Kuzhandaivel, Machine Learning-Based Prediction of Cyclic Voltammetry Behavior of Substitution of Zinc and Cobalt in BiFeO3/Bi25FeO40 for Supercapacitor Applications', ACS Omega 9 (31) (2024).
[163] Jens Peter Paraknowitsch, Arne Thomasa, Doping carbons beyond nitrogen: an overview of advanced heteroatom doped carbons with boron, sulphur and phosphorus for energy applications, Energy Environ. Sci. (10) (2013).
[164] S.B.S.M.J.K. Ken, O. Subrata Ghosh, Heteroatom-doped and oxygen-functionalized nanocarbons for high-performance supercapacitors', Adv. Energy Mater. (2020).
[165] R.S.A.M. A. A. E. C. M. F, P.A. Sachit Mishra, The impact of physicochemical features of carbon electrodes on the capacitive performance of supercapacitors: a machine learning approach, Sci. Rep. 6494 (13) (2023).
[166] X. Lu, C. Zhao, H. Tu, S. Wang, A. Chen, H. Zhang, Research on prediction of energy density and power density of biomass carbon-based supercapacitors based on machine learning, Sustain. Mater. Technol. 44 (Jul. 2025) e01309, https://doi.org/10.1016/J.SUSMAT.2025.E01309.
[167] H. Liao, et al., Machine learning prediction of supercapacitor performance of N-doped biochar from biomass wastes based on N-containing groups, element compositions, and pore structures, J. Energy Storage 100 (Oct. 2024) 113548, https://doi.org/10.1016/J.EST.2024.113548.
[168] Y. Sun, et al., Machine learning in clarifying complex relationships: Biochar preparation procedures and capacitance characteristics, Chem. Eng. J. 485 (Apr. 2024) 149975, https://doi.org/10.1016/J.CEJ.2024.149975.
[169] Tonio Buonassisi Juan Lavista Ferres, T. Keith, Butler Felipe Oviedo, 'Interpretable and Explainable Machine Learning for Materials Science and Chemistry, Acc. Mater. Res (2022) 597–607.
[170] S.L. B S. D. C. L. Y. S, H.L. Haiping Su, Predicting the capacitance of carbon-based electric double layer capacitors by machine learning, Nanoscale Adv. 6 (2019).
[171] X. Lu, C. Zhao, H. Tu, S. Wang, A. Chen, H. Zhang, Research on prediction of energy density and power density of biomass carbon-based supercapacitors based on machine learning, Sustain. Mater. Technol. 44 (Jul. 2025) e01309, https://doi.org/10.1016/J.SUSMAT.2025.E01309.
[172] X. Y. H, X.P. T. Y, Y.C.G.W. Liu, Machine learning modeling of the capacitive performance of N-doped porous biochar electrodes with experimental verification, Renew. Energy (2024).
[173] M. Rahimi, S.A. Salaudeen, Synthesis-feature-coupled machine learning approaches to predict the capacitance of biomass-derived carbon electrodes in supercapacitors, Mater. Chem. Phys. 348 (Jan. 2026) 131525, https://doi.org/10.1016/J.MATCHEMPHYS.2025.131525.
[174] A. Emad-Eldeen, M.A. Azim, M. Abdelsattar, A. AbdelMoety, Utilizing machine learning and deep learning for enhanced supercapacitor performance prediction, J. Energy Storage 100 (Oct. 2024) 113556, https://doi.org/10.1016/J.EST.2024.113556.
[175] A.G. Kusne, et al., On-the-fly closed-loop materials discovery via Bayesian active learning, Nat. Commun. 11 (1) (Nov. 2020) 5966, https://doi.org/10.1038/s41467-020-19597-w.
[176] X. Yang, C. Yuan, S. He, D. Jiang, B. Cao, S. Wang, Machine learning prediction of specific capacitance in biomass derived carbon materials: effects of activation and biochar characteristics, Fuel 331 (Jan. 2023) 125718, https://doi.org/10.1016/J.FUEL.2022.125718.